Environmental Earth Sciences (2020) 79:249
https://doi.org/10.1007/s12665-020-08984-7

ORIGINAL ARTICLE

The marble sculptures of General Bülow and Scharnhorst in Berlin: comparative, non-destructive analysis of the weathering state after 12 years of exposure

J. Menningen[1] · S. Siegesmund[1] · R. Krompholz[2] · Y. Rieffel[3]

Received: 8 August 2019 / Accepted: 1 May 2020 / Published online: 20 May 2020

Abstract
After almost 200 years of exposure, the monuments of General Scharnhorst and Bülow have been analysed by means of ultrasound. Both sculptures are made of Carrara marble, both sculptures have been exposed to the same environmental influences and both sculptures are, based on the results of the ultrasonic measurements, in alarming conditions. This statement can be made because of the data of three different measurement investigations within the last 12 years. In this short exposure time, the already low velocities have been reduced by 16.2% and 14.7%. The very low average velocity of 2.8 km/s for the sculpture of General Bülow and a slightly higher average velocity of 3.2 km/s for the Scharnhorst sculpture indicate that both sculptures are in a poor condition, even though a protective winter shelter has been used since 2004. Comparing tomographic velocity measurements performed in 2006 with the measurements made in 2018 was possible and showed that even areas with a thickness up to 90 cm show alarming low ultrasonic velocities down to 2.6 km/s. Even if the circumstances for both sculptures have been the same, they differ in their weathering state. The careful and transparent documentation of all measurements was in this context the most important aspect for the comparative studies. Irregularities in their weathering behaviour of the two statues can be distinguished, allowing an in-depth analysis of the deterioration of the marble.

Keywords Marble decay · Ultrasonic methods · Tomography · Non-destructive testing

Introduction

Crystalline marble shows a very special weathering behaviour in contrast to other natural stones. In addition to external environmental factors, the material properties of marbles have a significant impact with respect to the decay phenomena (e.g. Weiss 2002a; Zeisig et al. 2002; Koch and Siegesmund 2004; Scheffzück et al. 2007; Sáez-Pérez and Rodrígue-Gordillo 2009; Luque et al. 2011; Shushakova et al. 2013; Menningen et al. 2018a, b). The weathering of marble is usually a slow geological process, but fast enough for monuments to become damaged in less than a decade. An often discussed phenomenon is the complete structural destruction of marbles (e.g. Goretzki et al. 1987; Grunert 1988; Köhler 1988). Within the last several decades, the degree of marble deterioration has been determined by means of ultrasonic measurements. To determine the weathering state of culturally important objects made of marble, various studies have applied ultrasonic measurements (e.g. Köhler 1988; Dürrast et al. 1999; Weiss et al. 2001; Rüdrich et al. 2001a, b; Siegesmund et al. 2004; Ahmad et al. 2009; Snethlage 2014; Pascale and Lolli 2015; Babacan and Gelisli 2015; Mahmutoğlu 2017). The particular advantage of this method is its non-destructive nature; therefore, it is often used to characterise the in situ state of decay for free-standing sculptures, monuments, etc. The basic principle of this method is that an increasing crack growth and progressive opening of those cracks caused by weathering lead to a decrease of ultrasonic wave velocities. Köhler (1988) was able to demonstrate that the ultrasonic wave velocities are about 5 km/s for quarry-fresh marbles, but can drop to values of around 1 km/s for extremely damaged marbles. In 1978, a total structural collapse was noted for a marble sculpture made of Carrara marble that was protected under

✉ J. Menningen
johanna.menningen@uni-goettingen.de

[1] Geoscience Centre, University of Göttingen, Göttingen, Germany

[2] GEOTRON-ELEKTRONIK, Pirna, Germany

[3] Berlin Heritage Authority, Berlin, Germany

a pergola in the castle park of Sanssouci. On the basis of these observations, Köhler (1988) defined the concept of inner or core weathering as a special form of damage. He continued to address this hypothesis by determining significantly lower ultrasonic velocities at different depth ranges on a highly decayed marble capital from the Freundschaftstempel (Temple of Friendship) in Potsdam, Sanssouci, where he observed a higher variation in ultrasonic wave velocities. Based on many measurements, Köhler (1991) established a decay classification for marble, which connects decreasing compressional wave velocities with an increasing state of decay. This decay/velocity classification allows determining whether a marble sculpture can only be preserved by applying ongoing conservation measures. This is generally the case when the ultrasonic velocities for the compressional waves show magnitudes less than 3 km/s for most of the investigated directions (Snethlage et al. 1999; Siegesmund et al. 2004; Siegesmund and Dürrast 2014).

The marble sculptures of General von Bülow and von Scharnhorst are two important free-standing monuments of cultural heritage in Berlin, designed by Karl Friedrich Schinkel and realised by Christian Daniel Rauch. Because of their historical and cultural significance as creative work of these two famous representatives of German classicism, the sculptures have been investigated several times by ultrasonic measurements. The question arises, is further outdoor exposure of the two sculptures still possible, or should conservation measures be undertaken such as storage in a museum under controlled climatic conditions where they could be preserved for subsequent generations.

The state of weathering was investigated three times over a period of 12 years. The velocity data were used to constrain the strong degradation after this short period. Winter sheltering was implemented since 2004, for the last 3 years, the sculptures were permanently covered to protect them, so that moisture influences are negligible. Direct comparison of tomographic velocity measurements was made with those done in 2006 and the measurements performed in 2018, thus allowing an in-depth analysis of the deterioration of the marble.

Monuments of Scharnhorst and Bülow—historical background

The sculptures General Gerhard Johann David von Scharnhorst and Friedrich Wilhelm Freiherr von Bülow (Earl of Dennewitz) were placed beside the Neue Wache (New Guardhouse; Fig. 1) in 1822 in Berlin and unveiled on June 18, 1822. In 1950, both sculptures were removed from the Neue Wache and stored on the Museumsinsel (Museum Island), before the Scharnhorst sculpture was repositioned in 1961. While Scharnhorst was placed at the park on the opposite side of the Neue Wache, the von Bülow sculpture was kept in storage till 2002, due to political reasons. They underwent restoration in 1994 and were removed and put into storage in Berlin-Tegel. Since the 22nd of August 2002, they have been repositioned at the Prinzessinnengarten (Princesses Garden), where they have remained until now and aligned as they were at their original location by the Neue Wache.

Both monuments are made of Carrara marble, standing on a pedestal with reliefs and a plain marble base, which was renewed and reduced in height in the 1990s. The total height of both monuments is 5.2 m, while the sculptures are 2.7 m in height. Friedrich Wilhelm von Bülow (Fig. 2a) was one of the most successful Prussian generals during the Napoleonic wars and his sculpture presents him in an early nineteenth century general's uniform. Rauch chose a depiction of Bülow as a man of action with a self-confident appearance and a straight look to the left. Bülow's sculpture gazes toward the sculpture of General Johann David von Scharnhorst (Fig. 2b). He was a reformer of the Prussian army system and introduced compulsory military service, while his major efforts were focused on a liberal policy in the armed forces. The themes of combat and victory shown on the pedestal replicate the depictions visible at the triangular pediment of the Neue Wache (Fig. 1).

Within the last 200 years, both sculptures have undergone an assembly and dismantling history combined with vandalism and different measures of restoration, structural consolidation with an acrylic resin and cleaning. Since 2004, the sculptures are placed into an annual protective winter cover made of wood from November to April (see Fig. 2c). Inspection and maintenance are now periodically performed, which was initiated in 2009 by the Berlin Heritage Authority.

Experimental methods

Ultrasound

Ultrasonic data are calculated by the measured ultrasonic travel time determined for the respective measuring distance, considering the longitudinal wave. This type of wave correlates especially well with the structural properties of marble (e.g. Köhler 1991; Dürrast et al. 1999; Weiss et al. 2001; Rüdrich et al. 2001a, b) and depends on the mineralogical, physical and mechanical properties of the stone, its degree of water saturation and its level of deterioration.

Generally, for ultrasonic measurements, lower frequencies are used to measure opposite positions in transmission, mostly applied in cases where the reflection method will give qualitative insufficient results. The reasons for the insufficient quality can be found in the specific material characteristics. For example, the acoustic attenuation and sound

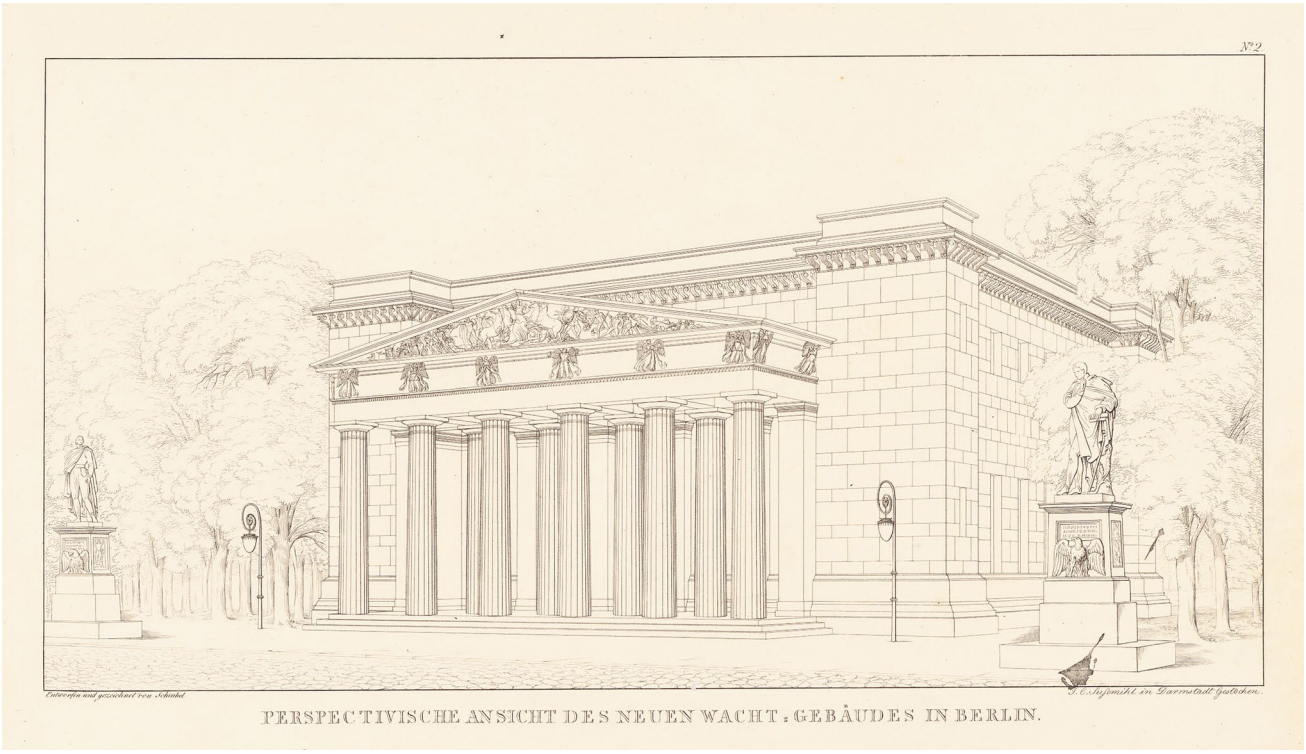

Fig. 1 Engraving of Karl Friedrich Schinkel's draft for the Neue Wache (Königswache) Berlin, 1858. In front of the neoclassical building, the monuments of General von Bülow and General von Scharnhorst are displayed in their primary location. (Schinkelzeichnung 1819 Karl Friedrich Schinkel (1781–1841)—Sammlung Architektonischer Entwürfe, Berlin 1858. TU Berlin Architekturmuseum, Inv. Nr. SAE 1858,002)

scattering are very high for heterogeneous material as natural stone and concrete. Therefore, low frequencies between 20 and 350 kHz are used for these materials, whereby the sound radiation is more or less unfocused, with an aperture angle of 180°. Ahmad et al. (2009) gives a more detailed overview regarding ultrasonic testing.

To determine the weathering state of important cultural and historical objects made of marble, the application of ultrasonic measurements has become established and ensures a non-destructive examination method (e.g. Köhler 1991; Dürrast et al. 1999; Weiss et al. 2001; Rüdrich et al. 2001a, b; Siegesmund et al. 2009; Köhler 2014; Snethlage 2014). The transmission method has been established as an often used monitoring examination; whereas, the tomographic approach is less often used (e.g. Cardarelli and de Nardis, 2001; Rüdrich et al. 2001b; Siegesmund et al. 2009; Capizzi et al. 2013; Menningen et al. 2018a, b). The main reason that the conventional method is favoured is the very time-consuming tomographic measurement process and the non-trivial interpretation. While the transmission method considers the mean ultrasound travel time for one distance and gives no detailed information about the internal structure, the tomography allows the determination of the velocities in a cross-sectional plane. With an optimal ray coverage, the plane can be spatially resolved and corresponding weakness zones can be detected.

Ultrasonic tomography assumes that a longitudinal wave crosses on its way through an object the weathered surface, followed by the intact core, and then again the weathered surface on the other side. Assuming an equal weathering depth, the transit time of the P-wave will increase less than proportionately to the total thickness of the investigated object; so the average velocity will increase (see Blum and Rahm 1998). For an ultrasonic tomography on a predefined cross section, different measurement points are defined and marked. The transmitter is positioned at one defined point of measurement; while, the receiver is placed at each other defined point on that cross section. After completion of that array, the transmitter position is changed to the following defined point and the receiver is again positioned at each circumferential point, until the cross section is measured.

Textural analysis

Ultrasonic velocities are affected by material specific elements such as the fabric. The most important fabric elements

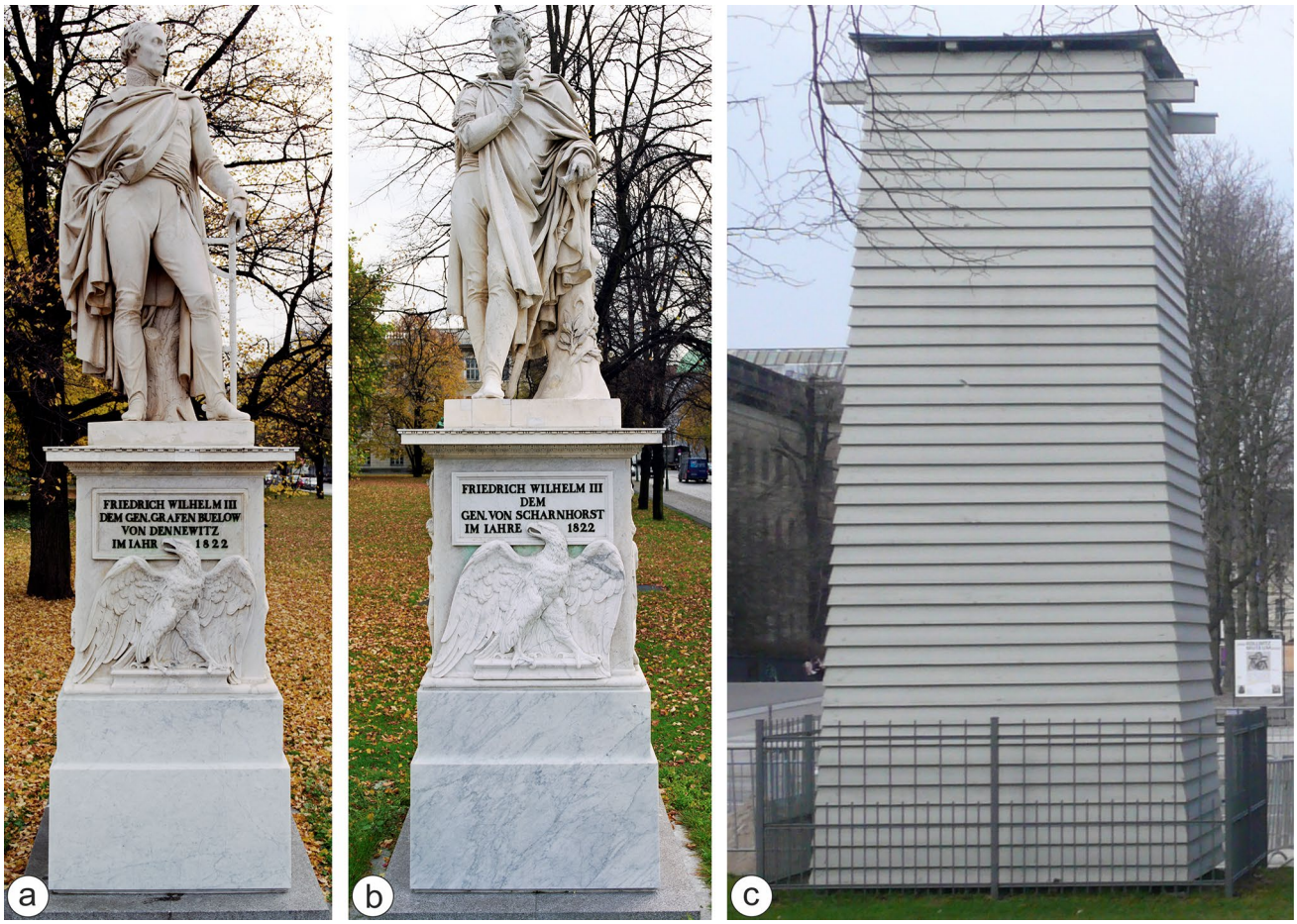

Fig. 2 Monuments of General von Bülow (**a**) and General von Scharnhorst (**b**) in their current appearance and **c** Sheltering of both monuments at their current location (Kai Zimmermann 2008)

are the lattice preferred orientation of the minerals (LPO), the existing microcrack populations, and the specific shape fabric, with grain size and grain shape preferred orientation. These fabrics are responsible for an anisotropy of the marble, expressed in the directional dependence of the elastic wave velocities. This means, for example, that the P-wave velocity shows different values when measured in different directions for the same rock sample (e.g. Khazanehdari et al. 1998; Wildhalm et al. 1999; Siegesmund et al. 1999; Rüdrich et al. 2001b; Weiss et al. 2002; Siegesmund and Dürrast 2014; Menningen et al. 2018a, b). This is caused by the anisotropic single crystal properties of calcite, which influence the ultrasonic velocity distribution (see Mainprice et al. 1990). To determine, whether there is a directional dependence influencing the velocity distribution of the marble sculptures, the crystallographic preferred orientation was analysed.

Therefore, electronic backscatter diffraction (EBSD) measurements were done on a piece of marble, taken from the drill core on the von Bülow sculpture to determine the LPO, which is also known as texture. EBSD is a texture analysing technique using scanning electron microscopy (SEM), where the SEM is equipped with an EBSD detector (for further information, see Wenk and van Houtte 2004, Maitland and Sitzman 2010).

General error analysis

Ultrasonic measurements are performed with the aim to get an insight into the structural properties of a material, including information about the weathering state as well as possible deterioration zones and cracks. From a technical point of view, several aspects need to be taken into consideration as they influence the ultrasonic results. First of all, coupling of the ultrasonic transducers to the respective surface is an important aspect. An adequate connection is fundamental for a high signal amplitude, which is necessary for an appropriate evaluation of the measurement.

Since the ultrasound velocity correlates with the rock fabric, extrinsic influences like decay phenomena connected

with granular disintegration are characterised by a decreasing velocity compared to the unweathered material. It should also be noted that quarry-fresh material shows intrinsic velocity variations. Responsible for these fluctuations are the specific bonding situations within the fabric as well as the properties of the respective mineral phases. The propagation of the sonic wave depends on the homogeneity of the material, whereby steel or water is ideal. Therefore, they show only small damping effects on the sonic wave. The more diverse the densities of involved material compounds are, the more the acoustic damping will increase, meaning the sound amplitude will decrease. If there is a density change between neighbouring compounds, the acoustic impedance will also change. The biggest impedance change occurs for a transition of solid state to air, as for example along a crack. Since dry coupling, meaning attachment of ultrasound probes with a plain surface without a coupling agent, will always cause a damping effect comparable to a crack, the application of a coupling agent is necessary. The thickness of this agent needs to fit to the surface conditions, but should generally be executed as thin as possible. Especially for important objects and sensitive surfaces, the choice of the coupling agent must be carried out carefully to avoid an irreversible pollution of them. Possibilities are the application of clay, which can be removed by a brush or plasticine covered with a foil; while any damping effect can be tested with a calibration standard.

Non-destructive ultrasonic measurement often forms the base for further investigations and decisions. Since the ultrasonic method indicates the degree of weathering, it is necessary to execute the analysis with a high degree of accuracy. The European standard EN 14576:2004 needs to be considered as well as the following aspects, where results are received with a reproducibility of less than 5% deviation (Köhler 2018).

The very common source of error is the instrument setting, especially an improper or broken cable and power supply as well as discharged batteries. These aspects influence the signal quality and, therefore, the exact determination of the travel time. The distance between emitter and transducer needs to be specified very carefully, (less than 1% deviation according to the EN), bearing in mind, that in coarse-grained materials, the distance needs to be approximately 10 times larger than the general grain size. Another aspect is the consideration of the relationship between measured distance and frequency, where the distance needs to be a multiple of the wavelength. The most frequent operation error is the wrong setting for the signal amplification, which needs to be properly scaled. Since the travel time is determined by the first arrival of the signal, wrong settings lead to undersized signals with a higher travel time or an overdriven signal resulting in a travel time which is too short.

These differences can sum up to a number of micro-seconds, which result in discrepancies particularly with regard to short measuring distances. Furthermore, the signal amplitude depends on the coupling to the surface (pressure and coupling agent), transducer arrangement (direct or indirect transmission) and choice of the right frequency, fitting the measuring distance, material damping or the presence of cracks and fabric decay.

A large influence on the velocities is caused by the presence of water in the measured object. The velocities of a deteriorated piece of marble can increase from 2.5 km/s up to 6 km/s, constituting a fresh, unweathered marble, caused by water saturation (c.f. Rüdrich et al. 2001b; Weiss 2002a,b; Siegesmund et al. 2009; Siegesmund and Dürrast 2014). Therefore, it is mandatory to ensure almost dry conditions before the ultrasonic measurements are taken. Otherwise, it is almost impossible to ensure a measured velocity which is not influenced by water saturation and it is necessary to assume lower velocities than the measured velocities.

Besides the described extrinsic effects, the intrinsic properties of the marble also have an effect on the measured velocities. The most important fabric elements are the crystallographic preferred orientation (CPO) or the lattice preferred orientation (LPO) of the minerals, the existing microcrack populations, and the specific shape fabric, with grain size and grain shape preferred orientation. These fabrics are responsible for a physical anisotropy expressed inter alia in the directional dependence of the elastic wave velocities. This means, for example, that the P-wave velocity distribution shows different values when measured in different directions for the same rock sample.

Results

Decay phenomena and rock status

Both sculptures consist of a whitish marble variety known as the Carrara type from Italy. Several types of decay phenomena are visible on the sculptures as shown in Fig. 3. Areas which are directly exposed to weathering influences, like arms, hands and garment folds show characteristic sugaring of these surfaces (Fig. 3a). These are highly pronounced for the left hand and arm of the Scharnhorst sculpture (Fig. 3b), where the original surface is almost completely lost. This pronounced surface roughness can be traced back to chemical solution processes, while less exposed areas show almost no alteration of the surface. In some cases, cracks can be found, which are visible due to the increased accumulation of dirt in those areas (Fig. 3c). Especially the garment folds show many black dots (Fig. 3d), which probably are caused by microbial growth and can be found more prevalently in the narrow gaps between the folds. Another phenomenon is an ochre coating spread all over the sculptures, as shown in Fig. 3e. The cause of this coloration is still under discussion

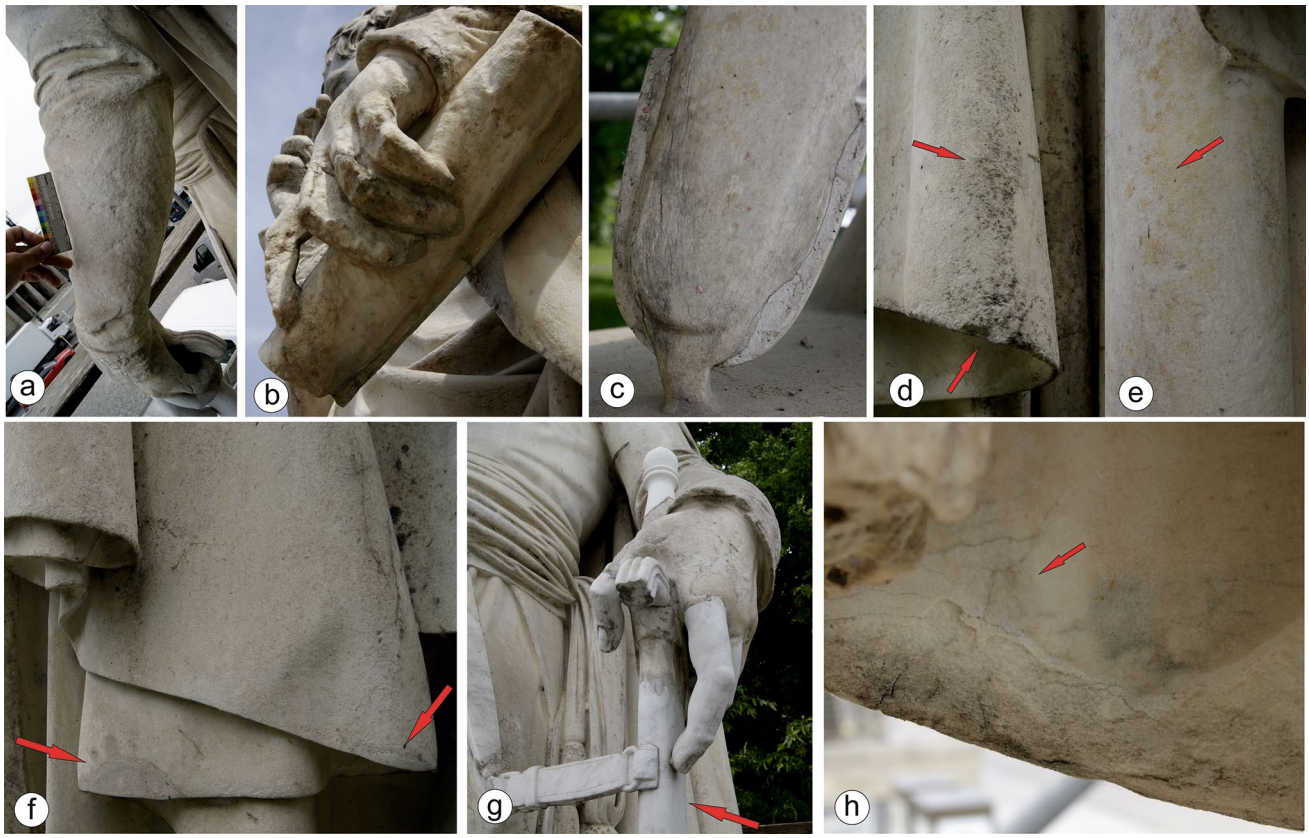

Fig. 3 Various decay phenomenon found at the monument of General von Bülow and Scharnhorst with **a** sugaring of exposed surfaces, **b** strongly weathered surfaces with sugaring of exposed surfaces, **c** cracks, **d** microbial growth, **e** discolouration, **f** lost material which was reconstructed by restauration mortar and **g** substitution made of marble and **h** Craquele on the surface

since it may be microbial growth or residues of former consolidation measures. Close examination needs to clarify this phenomenon. Several replacements of filigree parts can be found for example in the folds of the coat (Fig. 3f), where a restoration mortar was used to substitute the missing areas or (Fig. 3g) the total substitution by reconstructions made of marble. At the edge of Scharnhorst's coat, so-called Craquele can be observed on the surface, with a network of cracks; while the underlying fabric shows strong disaggregation (Fig. 3h).

The marbles show macroscopically a grain size of about 300 µm for General von Scharnhorst and about 200 µm for General von Bülow. A microscopic analysis by thin section was done for the sculpture of General von Bülow. The microfabric in Fig. 4a–d shows an inequigranular grain size distribution; while the grain shape is almost polygonal with interlobate to almost straight grain boundaries. Calcite is the main component of this marble, while accessory quartz and an opaque black mineral, probably graphite, can be found. To see if the fabric of the marble is deteriorated, the thin section was made using a blue coloured resin, to visualise open cracks and open grain to grain contacts. In Fig. 4, the left border of the images is parallel to the former surface of the sculpture, showing the fabric in a depth profile. Figure 4a and c shows that small cracks (marked with red arrows) run along the grain boundaries and can primarily be found between the grain to grain contacts, as so-called intergranular cracks. In Fig. 4c, an intragranular crack is observable, but this type of crack is less common. The crack distribution shows that they mainly occur in the first millimetres of the surface. They do not spread surface parallel, but slightly oblique into the depth of the drill core. Cracks at the outer areas of the drill core, parallel to the core should be disregarded, because they are caused by drilling and not related to weathering. Granular disintegration is observable in this core, but it is only weakly pronounced. Another important method for visualising these open grain boundaries is the use of scanning electron microscopy (SEM). SEM images were taken at a depth of about 4 cm (Fig. 4e) and at 6 cm (Fig. 4f) to the former surface. The grain contacts show no signs of granular disintegration at those depths.

Lattice preferred orientation

The analysed LPO, displayed as a lower hemisphere stereographic projection in Fig. 5a and b, can be described as

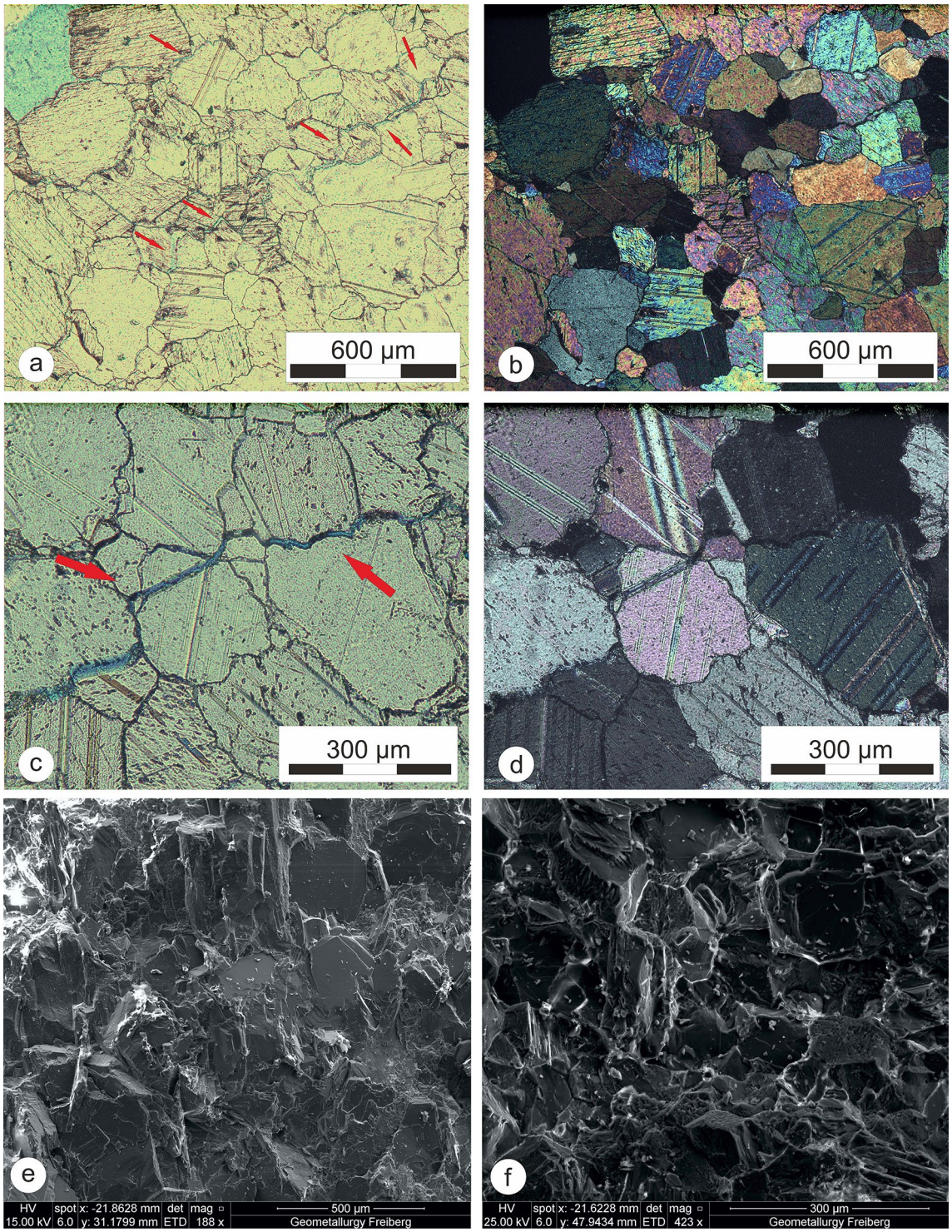

Fig. 4 Thin section images with coloured resin to visualise open cracks. The left rim of all pictures is parallel to the former surface of the sculpture. **a** polarised image showing the area close to the former surface, with slightly oblique cracks (red arrows) **b** cross-polarised image of the same region with the same magnification as (**a**); **c** detail of a crack system, showing intergranular cracks as the most common crack type, beside an intragranular crack, **d** image (**c**) under crossed polarizers, **e** scanning electron microscopy performed for a piece of the marble core taken from a depth of 4 cm and **f** 6 cm

an almost girdle like c-axis distribution with a low, elongated *c*-axes maximum intensity of 1.7 mrd (multiple random distribution) with an oblique orientation (Fig. 5a). The *a*-axes (Fig. 5b) show a great circle distribution surrounding the *c*-axis distribution with a maximum intensity of 1.4 mrd. The weak texture is typical for Carrara marble and has been analysed by different authors (e.g. Leiss and Ullemeyer 1999; Weiss et al. 1999; Rüdrich 2003; Rüdrich et al. 2013).

To see which amount of anisotropy for the ultrasonic velocity is controlled by the lattice preferred orientation, modelling of the intrinsic velocity distribution (see Mainprice et al. 1990) was performed using the Matlab-based software MTEX (see Hielscher and Schaeben 2008; Bachmann et al. 2010; Mainprice et al. 2011). To calculate the velocity distribution for the polycrystalline data, the measured texture data were used to calculate the intrinsic Vp distribution, based on the calculated ODF data. The modelled pole figure (Fig. 5c) shows a minimum velocity of 6.5 km/s according to the position of the c-axes maximum (see Fig. 5a), while the maximum velocity of 6.75 km/s is arranged along the a-axes maxima. The modelled intrinsic velocity distribution for this marble exhibits a low anisotropy of 3.7% assuming a crack free material. Many marble varieties with a strong crystallographic preferred orientation show a high anisotropy in their velocity distribution, which increases according to an increasing weathering state (e.g. Rüdrich et al. 2013). This effect needs to be considered for the interpretation of the tomograms (e.g. Cardarelli and de Nardis 2001; Rüdrich et al. 2001b; Menningen et al. 2018a, b).

On-site ultrasonic diagnostics

Field measurements in transmission

In May 2018, non-destructive ultrasonic measurements were applied to the sculptures, to form the basis for further investigations and decisions. Since the ultrasonic method indicates the degree of weathering, the ultrasonic measures were used in transmission and in the tomographic approach. Moisture has a huge impact on the ultrasonic velocity; therefore, it is necessary to ensure that longer dry conditions have existed before the velocities are measured. The sculptures were covered for almost 3 years (see Fig. 2c), ensuring a dry state for both sculptures. The night before the measurements were to take place, heavy rainfalls occurred in Berlin. Since the sculptures were wrapped in foil, and seemed to be dry in the morning, moisture influence should be negligible. However, at the pedestal and the head moisture influence cannot be totally excluded to affect the measured velocities.

The measurements were performed with a broadband transmitter, (UP-FH, for further information see www.geotron.de), where the necessary frequency could be chosen with respect to the measuring distance. Thus, one transmitter for all measurements could be used, which increases the accuracy as described before (see General error analysis).

Figure 6a shows the analysed velocities [km/s] measured for General von Bülow during transmission. Each value is colour coded for a specific state of weathering. The analysed compressional wave velocities range between 1.8 and 4.0 km/s, while the highest measured velocity (4 km/s) was detected at the replaced sword. The highest velocity for the original material is 3.5 km/s for his right foot. With 2.8 km/s, the average velocity is very low and is classified as granular disintegration. The overall measured velocities show a distribution that indicates a dependence on how exposed elements are and their geometry. The lowest and most alarming velocities classified as brittle are found at the filigree parts of the sculpture and at the completely exposed areas of the arm. Moreover, even thicker parts of the sculpture such as the trunk exhibit ongoing signs of deterioration with a velocity of 3.1 km/s.

Velocities measured for General von Scharnhorst (Fig. 6b) indicate a slightly better weathering state for this sculpture, with a maximum velocity of 4.1 km/s at the hip

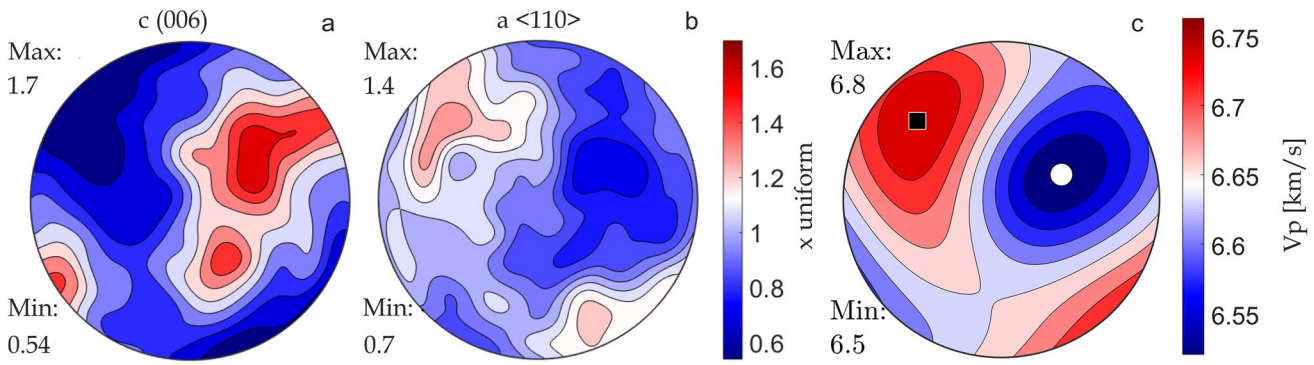

Fig. 5 Texture (LPO) given for **a** the c-(006) and **b** *a*-axes < 110 > . Intensities are given in mrd (multiple of random distribution), **c** 3D velocity distribution (km/s) modelled from the EBSD data of the sculpture von Bülow (lower hemisphere, stereographic projection)

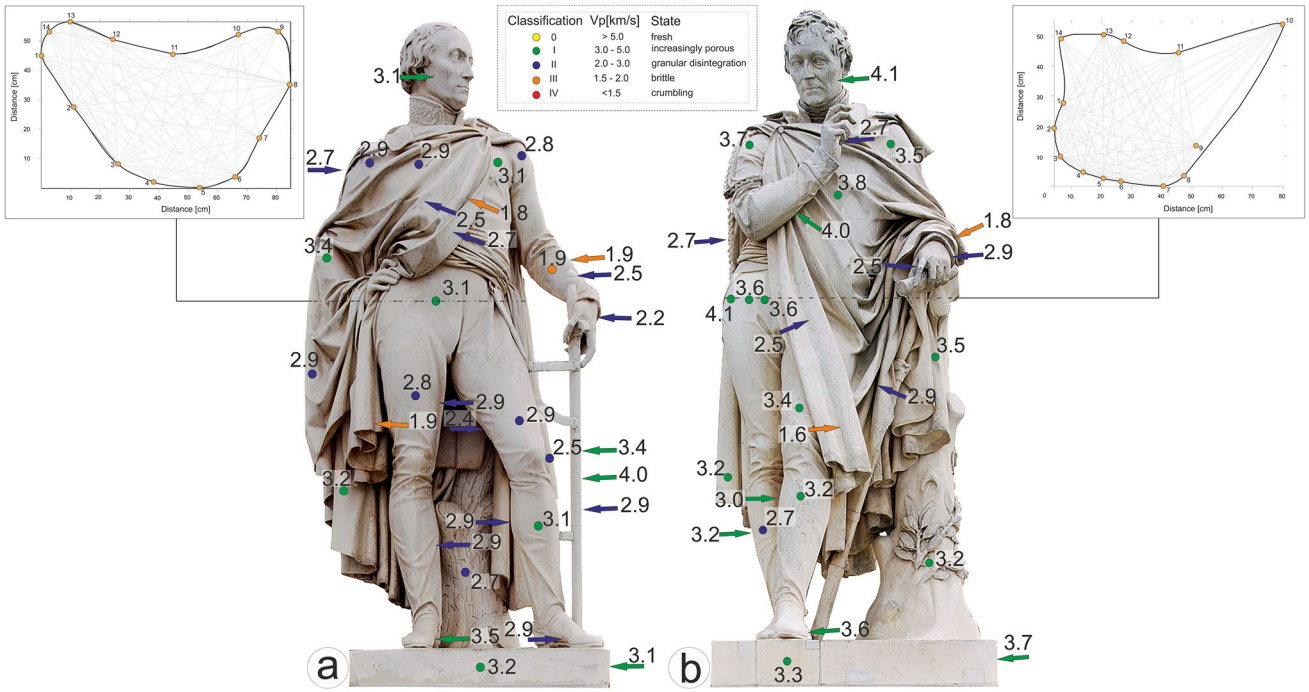

Fig. 6 Results of the ultrasonic transmission measurements performed in 2018 for General Bülow (**a**) and General von Scharnhorst (**b**). Arrows indicate the measurement direction from the left to right. Dots represent a transmission direction from the front to the back of the sculpture. The different colours represent the damage classification after Köhler 2018, displayed between the sculptures. Vertical sectional plane for the trunk is given for both sculptures

and head and the lowest measured velocity of 1.6 km/s at a garment fold. The mean velocity is, compared to General von Bülow, slightly higher with 3.2 km/s, reflecting the overall better conditions of this sculpture, 66.66% of the 27 measured velocities can be classified as increasingly porous. The geometry and exposition dependent velocity distribution as measured for Gen. von Bülow can also be observed for the Scharnhorst sculpture, while the thicker areas generally show higher values.

Ultrasound velocity and travel path

The velocities variate according to the length of the ray path. This path length varies between 3 and 64 cm for General v. Bülow, and 2 and 50 cm for General von Scharnhorst. To analyse what impact these lengths have on the velocities of the rays, they are plotted against each other in Fig. 7 (blue dots). Most velocities are analysed for ray paths between 2 and 20 cm, which range between 1.8 and 4.0 km/s for the first 10 cm, and 2.0 and 3.5 km/s for the distances between 10 and 20 cm for Bülow (blue dots in Fig. 7a). The velocities determined for the distances above 20 cm show a less strong variation of the values with velocities between 2.7 and 3.4 km/s. The velocities at short travel paths vary more strongly, while velocities at longer ray paths vary less. However, the number of longer travel paths is relatively low. Nevertheless, this velocity variation is not uncommon for weathered marbles and is a logical consequence of deterioration and the low probability that a short ray path will cross unweathered material; whereas, long travel paths almost always pass weathered and unweathered, or low weathered, areas of the stone (Blum and Rahm 1998, Siegesmund et al. 2004). In comparison, for the General Scharnhorst sculpture (blue dots in Fig. 7b), fewer determined velocities are in the class granular disintegration. The weathering state is better than the sculpture of Bülow, but the velocities are low as well. The variation of velocities with a short ray path, smaller than 10 cm, is with 1.7–3.2 km/s lower than for the Bülow sculpture; while, they vary between 2.7 and 4.1 km/s for distances between 10 and 20 cm, which is higher than the values measured for Gen. Bülow. The longer ray paths also show a smaller range for this sculpture, while the variation within these distances is between 3.4 and 3.8 km/s. Therefore, both sculptures have a comparable weathering state, while the sculpture von Scharnhorst shows higher velocities considering the long travel paths, which is reflected in the slightly higher mean velocity of 3.2 (±0.62) km/s compared to the 2.8 km/s (±0.45) for Gen. v. Bülow. Both sculptures have suffered during the last decades; while General v.

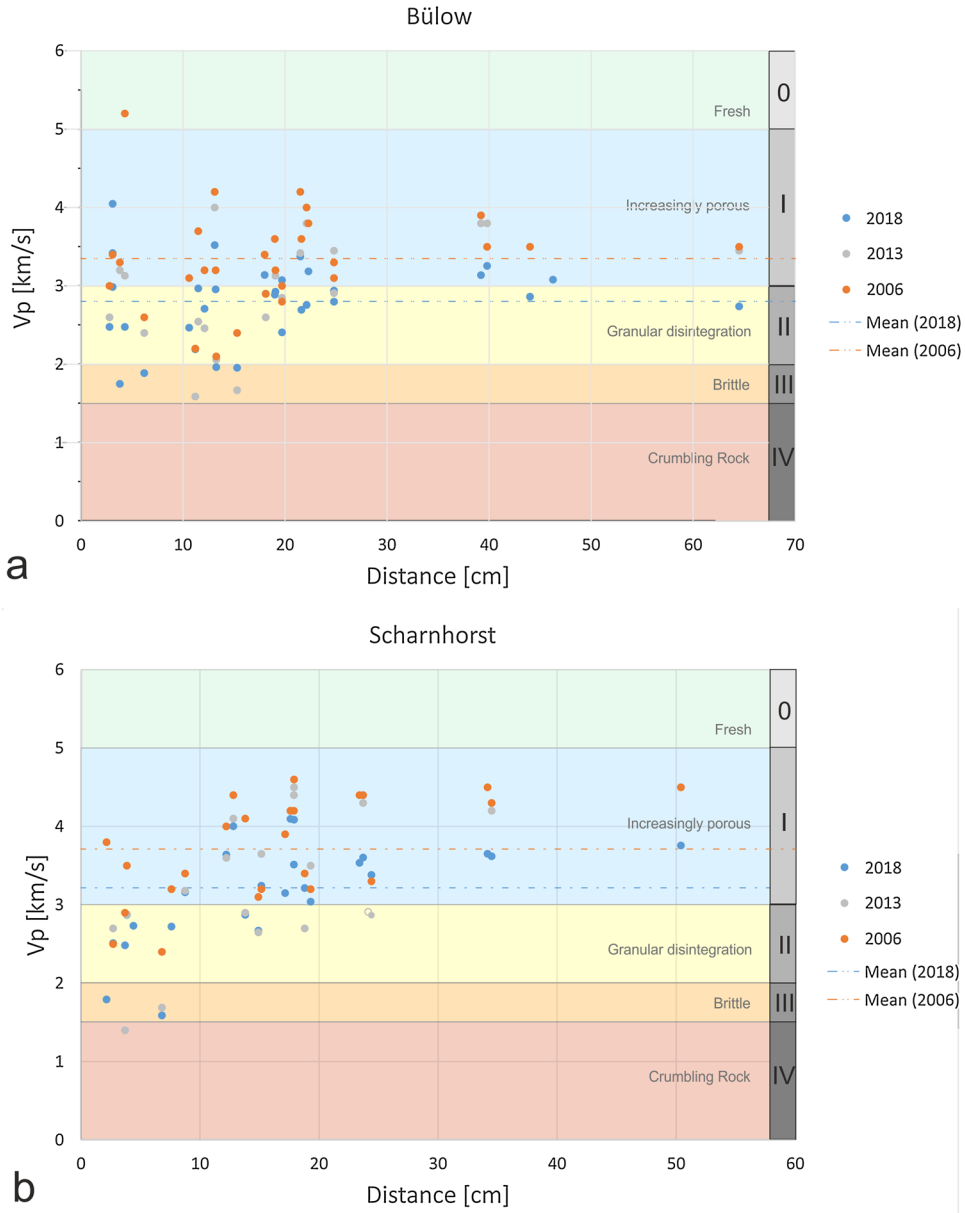

Fig. 7 The measured transmission velocities (km/s) of von Bülow (**a**) and von Scharnhorst (**b**) plotted according to the distance (cm) the ray needed to travel. The dashed line represents the average velocity

Scharnhorst shows a lower state of deterioration, even if the Bülow sculpture was less exposed to the environment.

Transmission velocities only reflect the mean value for the measured distance and give no information about the inner structure. In addition, ultrasonic measurements have been performed in a tomographic application. The measurements were executed at the trunk in the middle of both sculptures at a height of about 1.4 m above the pedestal (see Fig. 6) for 14 different measuring points, with 91 measured travel paths.

Ultrasonic tomography

The 2D tomographic analyses was done using the software GeoTomCG, which uses an inversion calculation based on SIRT (simultaneous iterative reconstruction technique). For further information about the software, see GeoTom, LLC, 2017. To process the data, the measured minimum and maximum values, received for the tomographic plane, have been used as a limiting factor. The initial velocity model has been calculated based on the average velocity. These processed tomograms are transferred to the programme Surfer and are depicted as contour plots in Fig. 8, where the lower margin of both plots refers to the front of the sculptures (north is the viewing direction), while the upper margin refers to the back.

The tomogram calculated for General v. Bülow (Fig. 8a) shows a small channel of lower velocities (2.5–2.8 km/s) in the middle of the sculpture that are elongated to the west. The low velocities in the western part of the tomogram are

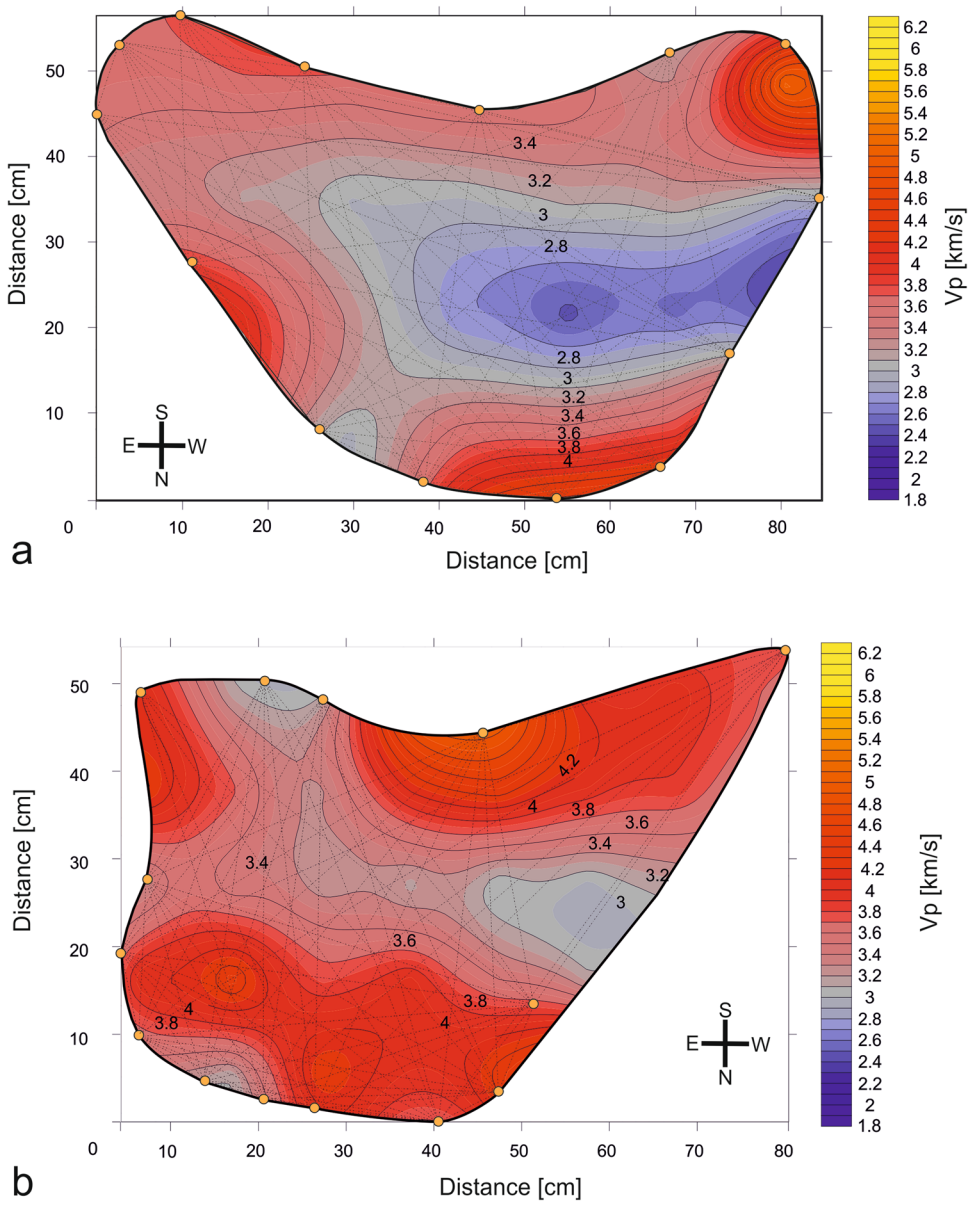

Fig. 8 Ultrasonic tomograms of General v. Bülow (**a**) and General v. Scharnhorst (**b**), computed for the horizontal sectional planes shown in Fig. 7. Velocities are given in km/s, the compass direction is given in the left (**a**) and right (**b**) corner of the plot. The lower edge of both tomograms represents the front view of both sculptures

in an area with low or no ray coverage. The highest velocities can be found in the northern direction, which is the front of the sculpture. The higher ultrasound velocities are arranged like a "U" dipping to the west, surrounding the low east–west striking velocity channel. The majority of the tomogram is characterised by velocities between 2.8 km/s and 3.6 km/s; the highest values can be found selective along the rim of the tomographic plane. This area needs a sensitive and careful interpretation because the number of rays, travelling this area is very low. The tomogram displayed for General v. Scharnhorst (Fig. 8b) shows fewer areas with lower velocities where values range between 3.0 and 5.0 km/s. The small zone in the western part of the tomogram is again an area with low ray coverage. The highest velocities can be found in the northern part of the tomogram; while the lower velocities run through the tomogram as a belt in the middle of the tomographic plane, striking east–west, further as an area in the north-east and south-east of the tomogram. Most areas of the tomogram show velocities between 3.4 and 4.2 km/s, confirming the transmission measurements, that this sculpture is in a slightly better state of condition than v. Bülow.

Discussion

Ultrasonic measurements can provide a non-destructive insight into the structural properties of a material. In the case of objects of cultural heritage, urgent attention is given to the weathering state as well as possible deterioration zones and cracks. This method is proven and

powerful, but some basic knowledge is indispensable for accurate velocities and a competent interpretation. Based on this method, decisions regarding conservation and restoration measures can be made, as well as the highest impact decision, the replacement of important sculptures.

In 2018, fortuitous circumstances allowed the comparison of the present results with the velocities acquired in 2013 and 2006 for the sculptures von Bülow and von Scharnhorst. This has given the present study an opportunity for a closer examination of the development of deterioration within the last 12 years. Due to the good documentation of those investigations, most boundary conditions are known, e.g. the equipment used, measured areas and the exact distances between transmitter and receiver positions. This improves the comparability of those studies with the latest results. Even if technical conditions, application errors and the possible deviation of 10% between different measurement teams (see DBU final report AZ. 29544/01) influence the results and consequently the comparability of different measurements, the highest impact causing deviations, is given by possible water saturation.

Ultrasonic velocities of marbles strongly depend on the moisture content of the rock. Marbles can show velocities of 3.0 km/s and less in the dry state; while velocities may reach about 6.0 km/s under water-saturated conditions (Rüdrich et al. 2001a; Weiss et al. 2002a; Siegesmund et al. 2009; Menningen et al. 2018b). The pore space developing in marbles is small but very efficient in reducing the velocities and also increasing them due to fluid saturation. Therefore, ultrasonic velocity measurements are extremely sensitive on type and degree of fluid saturation (see Weiss et al. 2002a).

Before the measurements were done in 2018, the sculptures had been covered for about three years. This means both sculptures were protected from the rain, with the exception of the aforementioned rainfall the night before measuring, and thus can be considered dry. The investigations in 2006 and 2013 were executed after 2 weeks of coverage, while the exact date is not known. In 2006, the measurements were done in November, after 3 months of restoration, when besides different measures, a structural strengthening was performed with the application of 3% Paraloid B72 (Acrylic resin) in acetone to both sculptures. Two weeks before the ultrasonic measurements were done, the sculptures have been completely covered against direct rainfalls. In September and October 2006, 16 days with rainfall have been reported. The amount of precipitation has been low, while the 29th of October showed a higher amount of rain with 13 mm (see https://www.wetteronline.de/, data for Berlin-Tegel in 2006). Therefore, the influence of water cannot be absolutely excluded, but should be not that high.

Comparative investigations

Field measurements in transmission

The applied transmission measurements executed in 2018 were done at the same locations on the sculptures as in the former investigations. Thus, the results of 2018 can be compared to them and give an impression about the damage influences on the sculptures within the last 12 years. In 2006 and 2013, the measurements were executed with a 250-kHz transmitter on the filigree parts and 48 kHz for the pedestal. In contrast, the 2018 study used a broadband transmitter, so that one transmitter could be used for all measurements, which increases the accuracy as described in the section general error analysis.

Figure 9 shows the measured velocities [km/s] received for General von Bülow in 2006, 2013 and 2018. The velocities for most parts of the sculpture slowed down during the investigated timespan and changed from the classification of increasingly porous (green) to granular disintegration (blue). The maximum velocity in 2006 was measured on a part of the substituted sword handle with 5.2 km/s. While the handle slowed down to 2.5 km/s, the highest measured velocity (4 km/s) was in 2018, detected on the substituted sword. As this was an additional measurement, no correlating value with the study in 2006 exists. The maximum velocity measured for the original material in 2006 was 4.2 km/s, in comparison with the maximum of 4.0 in 2013 and 3.5 km/s in the present study. The lowest velocity measured in 2006 was 2.1 km/s for the left arm, which showed no reduction in 2013 and slowed down to 1.9 km/s in 2018. The lowest velocity in 2013 measured on the left hand was 2.2 km/s, which is the same in 2018 as in 2006. In 2018 the lowest velocity detected was on a mantle fold with 1.8 km/s, which was much higher in 2006 (3.3 km/s) and 2013 (3.2 km/s). The mean velocity was 3.4 ($\pm$0.62) km/s in 2006, 3.0 ($\pm$0.67) km/s in 2013 and has decreased to 2.8 ($\pm$0.46) km/s in 2018, which is a reduction of 15.7% during the last 12 years and 5.7% within the last 5 years.

Figure 10 displays the velocity evolution for the sculpture General von Scharnhorst using the same classification and colour code as in Figs. 6 and 9. In 2006, the velocities indicate a slightly better weathering state for this sculpture with a maximum velocity of 4.6 km/s and a minimum velocity of 2.4 km/s; whereas the velocities received in 2018 at the same position are now reduced to 4.1 km/s (max) and 1.6 km/s. They remained almost stable until 2013. The mean velocity decreased from 3.7 ($\pm$0.63) km/s in 2006 down to 3.4 ($\pm$0.88) km/s in 2013 and 3.2 ($\pm$0.62) km/s in 2018. The velocity reduction is about 14.7% within the last 12 years and 5.1% since 2013. The sculpture of Gen. v. Bülow shows a higher decrease of the ultrasonic values and that the deterioration is constantly increasing, independent

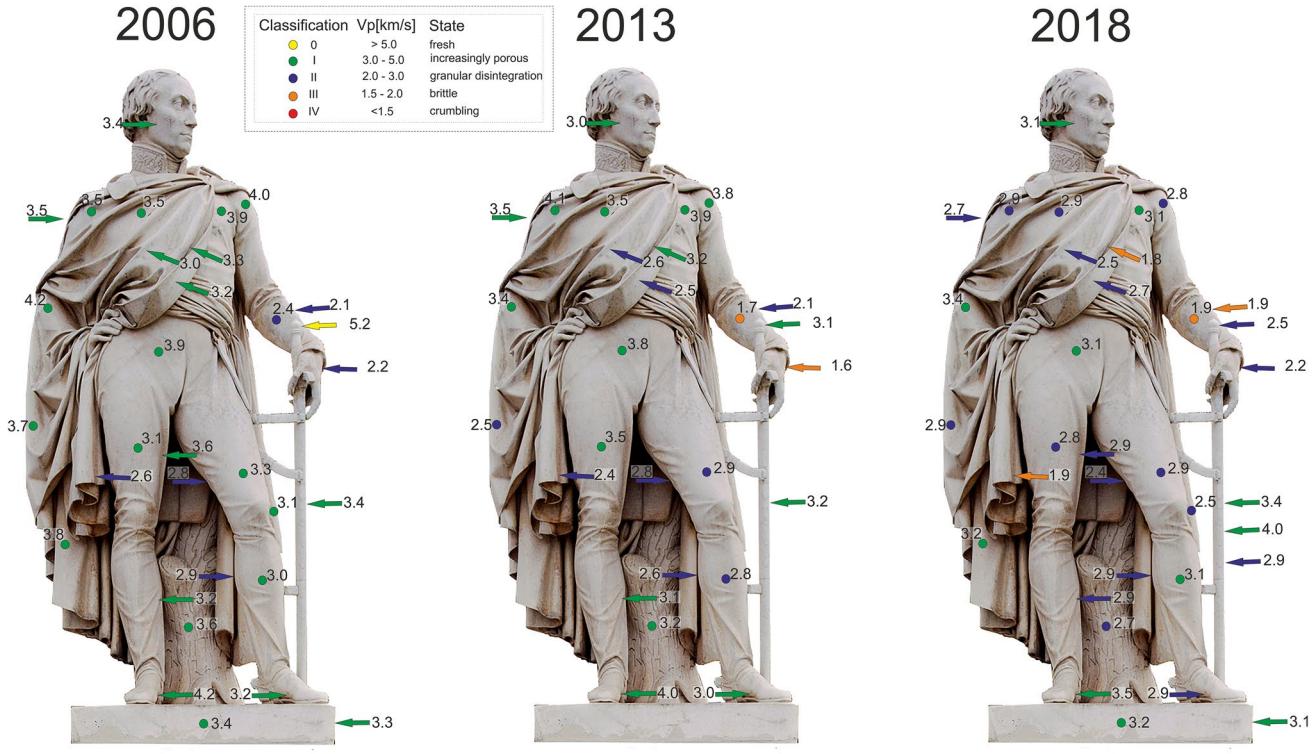

Fig. 9 Measured ultrasonic velocities, analysed using the pulse transmission technique, given for the sculpture of General v. Bülow in 2006, 2013 and 2018. Arrows indicate a lateral (east–west) attachment of the probes, while the dots represent the north–south direction of the arranged probes. Colour code represents the damage classification modified after Köhler 2018. Numbers give the measured velocities in km/s

of the preventive measures applied within the last 15 years. Especially the filigree parts such as folds, and completely exposed areas show the lowest and alarming velocities which need to be classified as brittle.

To analyse what impact the path lengths have on the velocities of the rays, they are plotted against each other for General von Bülow in Fig. 7 a. Most velocities are analysed for ray paths between 2 and 20 cm, which ranged in 2006 (orange dots) between 2.6 and 5.2 km/s for the first 10 cm and between 2.1 and 4.2 km/s for distances between 10 and 20 cm. In 2018 (blue dots), these values are lower with 1.8–4.0 km/s for the first 10 cm and 2.0–3.5 km/s for the distances between 10 and 20 cm. The velocities determined for the distances above 20 cm show a less strong variation of the values with velocities between 3.1 and 4.2 km/s in 2006 and 2.7 and 3.4 km/s in 2018. The velocities at shorter travel paths vary more strongly, while velocities at longer travel paths vary less. If the velocities of the last three studies are compared (Fig. 7a), the ultrasonic velocities measured for General v. Bülow generally slowed down throughout the last 12 years and the most common damage classification changed from increasingly porous to granular disintegration. In comparison, fewer velocities examined for General Scharnhorst are located in the classification granular disintegration (Fig. 7b) and the weathering state can be described as better than the sculpture of Bülow, but the velocities are also low and decreased within the last 12 years. The variation of velocities with a short ray path, smaller than 10 cm is with 2.4 and 3.8 km/s lower than for the Bülow sculpture. They vary between 3.1 and 4. 6 km/s for distances between 10 and 20 cm in 2006, which is higher than the values received for Gen. Bülow. In 2018 (blue dots), these velocities are slower with 1.7–3.2 km/s for the first 10 cm and 2.7–4.1 km/s for the distances between 10 and 20 cm. The longer ray paths also show for this sculpture a smaller range, while the variation within these distances was higher in 2006 (3.3–4.5 km/s) and is now between 3.4 and 3.8 km/s. Therefore, both sculptures have a comparable weathering state, while the sculpture von Scharnhorst shows higher velocities considering the long travel paths, which is reflected in the slightly higher mean velocity of 3.2 ($\pm$0.62) km/s in 2018 compared to the 2.8 ($\pm$0.46) km/s for General v. Bülow. Both sculptures have deteriorated during the last decades, however the General v. Scharnhorst sculpture shows a lower state of deterioration, even if this sculpture was longer exposed to environmental influences as v. Bülow.

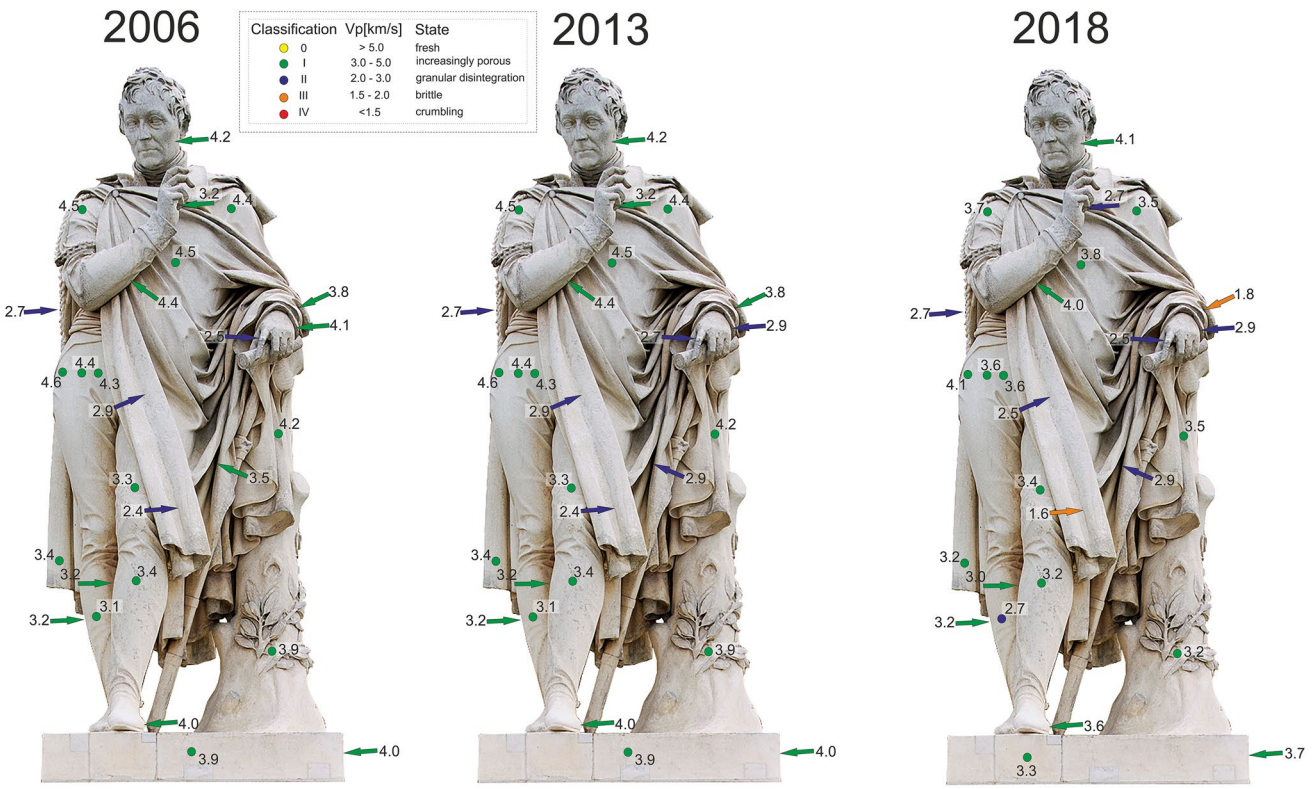

Fig. 10 Measured ultrasonic velocities, analysed using the pulse transmission technique, given for the sculpture of General v. Scharnhorst in 2006, 2013 and 2018. Arrows indicate a lateral (east–west) attachment of the probes, while the dots represent the north–south direction of the arranged probes. Colour code represents the damage classification modified after Köhler 2018. Numbers give the measured velocities in km/s

Laboratory measurements

To see if the distribution of velocities shows any directional dependence, a drill core from the General v. Bülow sculpture was analysed by ultrasonic measurements. The drill core was examined as a depth profile along the 10-cm drill core with incremental measuring points of 1 cm, starting close to the former surface of the sculpture at 1 cm and ending at 9 cm from the end of the core. The depth profile has been measured in two different directions (Fig. 11 red and blue graph). A third direction (green graph) represents the value determined for the whole length of the core. Reorienting the core to the compass direction of the von Bülow sculpture, the blue line represents measurements in the east–west direction, whereas the green graph is oriented to the north–south direction. Therefore, the blue and green graphs in Fig. 11 depict the velocities measured in the horizontal orientation, equivalent to the horizontal in the sculpture, while the red graphs depict the vertical orientation. The measurements were done under dry (marked with a square) and water-saturated conditions (marked with a circle). The results obtained for the core are depicted in Fig. 11 and show an interesting trend for the values under dry conditions. Contrary to the expected trend, the velocities taken at the surface of the core are higher than the values at a depth of 9 cm. The velocities are 4 km/s for the first centimetre and slow down to 3.1 km/s within the first 3 cm; while, the last 6 cm shows a small range within the velocities around 2.7 and 3.2 km/s. The velocity for the whole length of the core is 3.4 km/s. Based on these data, a directional dependency cannot be detected. This can be caused by a low pronounced preferred orientation as shown in Fig. 5a and b or because the measurements have been executed at intermediary areas and missed the preferred directions. The velocities under water-saturated conditions show a comparable distribution for the blue graph, measured in the east–west direction, with little higher values between 3.7 and 4.7 km/s compared to the results for the dry sample ranging between 2.6 and 4.1 km/s.

Both graphs show higher velocities at the surface and lower velocities at a depth of 9 cm. The red graph shows the fastest velocities, which were measured under water-saturated conditions in the vertical direction. The velocities increase from 5.1 km/s up to 5.7 km/s for the first two centimetres, before they decrease down to 4.3 km/s until a depth of 8 cm, where the velocity finally increases for the last centimetre, up to 5.4 km/s. This behaviour can also be

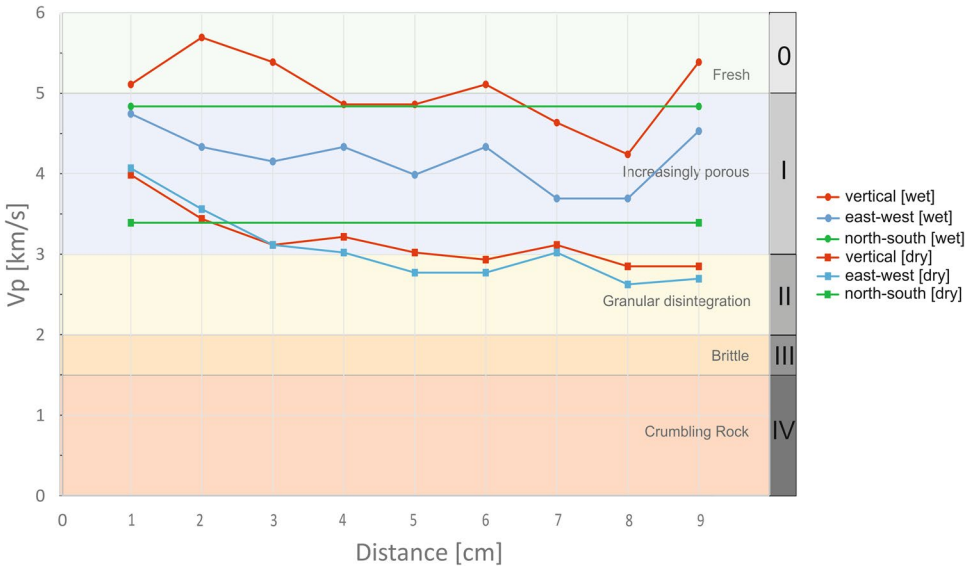

Fig. 11 Ultrasound velocities measured for a drill core from the von Bülow sculpture under dry (square markers) and wet conditions (dots). The green line represents the velocity investigated for the whole length of the core, according to the north–south compass direction. The red and blue values were received in the horizontal east–west direction (blue) and vertical direction (red). The measurements were executed as a depth profile, 1 cm is almost the former surface of the sculpture and 9-cm depth into the sculpture. Velocities were measured with a distance of 1 cm between the measuring points

observed for the blue graph under water-saturated conditions, which increases from 3.7 up to 4.5 km/s. The value for the north–south direction of the core is again within the range of the other two directions. The values suggest that there is a directional dependence of the ultrasound velocities, but these results do not seem to be reliable. In many studies of ultrasound velocity distribution and their development due to weathering, the variation in different directions increases with increasing deterioration, expressed in a higher anisotropy. Therefore, the core shows a contrary trend, with less anisotropy within the different directions in a deteriorated state. It seems to be more plausible that other effects influence these results. The core has a diameter of 20 mm, which triggers different problems that need to be considered. First, a relatively small change in the short travel time will cause a large change in velocity, which is caused by the relationship of travel time and velocity. Second, the small diameter combined with a big length of the core causes a fast drying of the water-saturated sample. Therefore, the difference between the horizontal and vertical direction under saturated conditions can be influenced by the drying process. Third, the small diameter combined with the frequency of 350 kHz and the chosen probe tip can cause wrong results, especially for the high velocities. Based on the correlation of frequency and wavelength (see Deutsch et al. 2002), the wavelength caused by the specific wave velocity–frequency combination can be determined. In this study, all wavelengths show sufficient sizes, but nonetheless the diameter of the sample is very small and could influence the results.

Generally, the velocities measured for the core are low and can be classified as granular disintegration (see Fig. 11); while at the SEM pictures, taken at a depth of 4 cm (Fig. 4e) and at 6 cm (Fig. 4f), the marble shows no open grain boundaries. The reasons for higher values, analysed for the surface could be a former consolidation. In 2006, a consolidation with Paraloid B72, an acrylic resin, was mentioned in the restauration history provided by the Berlin Heritage Authority.

Ultrasonic tomography 12 years later

In Fig. 12, the Vp-travel path plots are given for the velocities determined for the tomographic planes for both sculptures in 2006 and in 2018. In 2018 they range between 2.3 and 5.1 km/s for General v. Bülow (Fig. 12a, blue dots) with an average value of 3.3 (±0.44) km/s, while they are slightly higher for General v. Scharnhorst and range between 2.6 km/s and 5.1 km/s with an average value of 3.8(±0.43) km/s (Fig. 12b, blue dots). The Vp-travel path plot shows, according to the transmission measurements described before, generally lower velocities for Bülow, with a broader range of them, even for long distances; while the variation is lower for the long distances of General v. Scharnhorst. Even if both sculptures exhibit ultrasound velocities that can be classified as increasingly porous, the slightly better conditions of General von Scharnhorst, with fewer values in the category of granular disintegration can be observed easily in Fig. 12.

Independent of the length of the travel path, all measured the velocities continued to decline since 2006. The mean velocity of 4.0 (±0.5) km/s declined around 0.7 km/s down to 3.3 (±0.44) km/s in the last 12 years for General v. Bülow and around 1.0 km/s from 4.8 (±0.5) km/s down to 3.8 (±0.43) km/s for General v. Scharnhorst**.** The most astonishing result is that even the velocities for long distances of more than 40 cm show a significant reduction of about 1 km/s, indicating a strong deterioration. Another

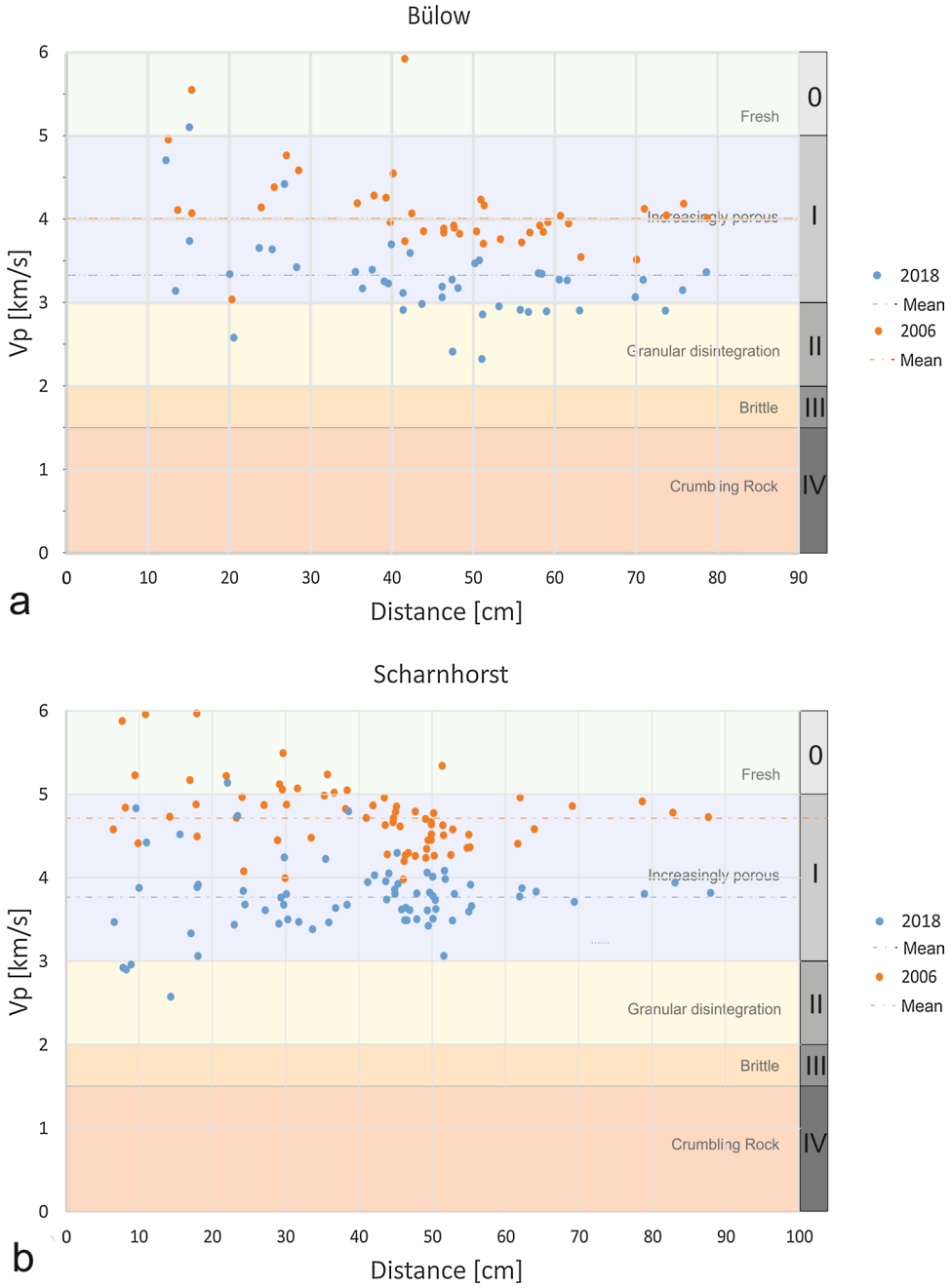

Fig. 12 Measured ray velocities (km/s) of the tomogram for von Bülow (**a**) and von Scharnhorst (**b**) in 2018 (blue dots) and 2006 (red dots) plotted according to the distance (cm) the ray needed to travel. The dashed line represents the average velocity

interesting aspect is that all velocities for the shorter distances of General v. Bülow are the same or higher than the values for longer distances. Higher velocities are not uncommon for shorter distances and can be caused by different reasons (e.g. Lindner et al. 1999), but that more or less all measured velocities for short distances of a weathered marble are higher than those for longer distances is quite unusual (e.g. Fleischer 2002; Rüdrich et al. 2013).

Besides the transmission measurements, a 2D tomographic reconstruction was done for both sculptures in 2006. Since this measuring investigation was well documented, it was possible to choose in 2018 the same height and transmitter–transducer positions as in 2006. Consequently, it was possible to compare the tomograms of 2018 with the tomograms of 2006. An exception is that the better ultrasonic probes in 2018 enabled to detect more signals than in 2006**.** As a result, the tomograms of 2018, used for the comparison of both investigations and modelling ΔVp, have been reduced to the same amount of measuring points as in 2006. This leads to 41 measured rays for the sculpture General von Bülow and 73 measured rays for General von Scharnhorst.

The tomographic data of 2006 were used to model tomograms and to compare them to the tomograms of 2018, for a

better interpretation of the alterations that occurred within the last 12 years. Due to the smaller number of measured velocities in 2006, the ΔVp tomograms have been modelled with the same number of travel paths for the 2018 tomograms (small tomograms in Figs. 13 and 14b). Nevertheless, the tomograms for General von Bülow shown in Fig. 14 demonstrate that the distribution of the velocities in 2006 is comparable to the 2018 data set with significantly lower values, regarding their spatial arrangement. Both tomograms show low velocities in the middle of the tomograms with 3.5 km/s in 2006 (a) and 2.5 km/s in 2018 (b); while, the outer part shows higher velocities ranging between 4.2 and 4.8 km/s in 2006 and 3.4 km/s and 4.0 km/s in 2018. The higher number of measured rays reveals that, in 2018, the low velocities in the middle expand to the western surface. Disregarding the additional rays as shown in the small tomogram, this area is invisible, according to the 2006 tomogram.

The Δ-Vp tomogram shown in Fig. 13c depicts that the highest reduction occurs in the eastern part and the middle of the tomographic plane, separated by an area with less reduction, tending to the south, the back of the sculpture.

The tomograms for General v. Scharnhorst, depicted in Fig. 14 show a different distribution. Here, the velocities in 2006 (a) ranged between 4.2 and 6.2 km/s, while the zone in the south-west showing high velocities was only passed by a few crossing ray paths; therefore, this area should be interpreted with care. The velocities of 2018, shown in Fig. 14b, are lower than in 2006 (a), but unlike the tomograms of General v. Bülow, the reduction is primarily located at the outer areas of the sculpture. The Δ-Vp tomogram in Fig. 14c shows that the eastern and western areas are stronger deteriorated than the middle, where the reduction was not that high.

The distribution of the ultrasonic velocity depends on the lattice preferred orientation. Therefore, the modelled three-dimensional ultrasonic velocity for the sculpture of General von Bülow (see Fig. 5c) was rotated about 90° (Fig. 15) to have the same orientation as the two-dimensional tomograms (Fig. 13). The displayed velocity is given at the lower hemisphere and cannot be directly transferred to the measured layer in Fig. 13, as they show different dimensions. Nevertheless, the area of low velocities in Fig. 13 could be influenced by the texture, while an isotropic velocity distribution could also be possible. Since the two-dimensional velocity distribution for the specific section could not be determined, no clear determination of the intrinsic velocity distribution can be given for the specific tomographic section. The amount of decay phenomena and heterogeneities can only be quantified if the anisotropic velocity variation is considered. But as the texture is only weakly pronounced and even the measurements at the drill core showed no clear directional dependence, the influence based on anisotropy seems to be negligible.

Another aspect which influences the damage and the spatial distribution is the geographic exposure of the sculpture (see Brimblecombe 2014). The western area is the main weather side in Berlin (see www.de.windfinder.com). The long time span of outside exposure indicates that the main influence on the rock fabric is caused by weathering. Since the main wind direction is west, the impact of weathering should be more pronounced for the west-facing surfaces. Decay caused by cyclical influences of wind, wind-driven rain and other changes of humid and dry conditions should be most pronounced on these sides of the sculptures.

Conclusions

After almost 200 years of exposure, several relocations, vandalism and restauration measures, the monuments of General Scharnhorst and Bülow have been analysed by ultrasonic measurements. The data of three different measurement studies in the last 12 years have been compared to describe the weathering behaviour of two important sculptures with a comparable weathering history. Both sculptures are made of Carrara marble, both sculptures have been exposed to the same environmental influences and both sculptures are, based on the results of the ultrasonic measurements, in alarming conditions.

The correlation of the dimension and the effective degradation mechanisms was described by Siegesmund et al. (2013). The filigree parts such as the folds and the completely exposed areas like the arms show generally the lowest and alarming velocities, which need to be classified as brittle. Due to the small dimension of these areas, the different degradation mechanisms lead to a very strong degree of decay. This can be confirmed by the results for both sculptures, but even thicker parts as the trunk exhibit ongoing signs of deterioration with velocities of 2.6 km/s for the sculpture of Bülow, signalling the advanced decay progress. Consistent with the results in 2006 and 2013, the sculpture of General v. Scharnhorst is in a better condition, compared to Bülow, but some conspicuous features need to be considered.

The transmission measurements from 2018 indicate that the filigree parts of both sculptures show lower velocities around 2 km/s, compared to thicker parts with velocities between 3 and 4 km/s. The velocities analysed for the first 10 cm vary much more for General v. Bülow than for General v. Scharnhorst. Generally, since 2006 the reduction is higher for Bülow than for Scharnhorst.

The direct comparison of the velocity reduction for each measured point since 2006, displayed in Fig. 16, shows that the transmission measurements (yellow dots) performed for Bülow (a) show a high reduction for short paths and a lower total reduction for longer distances. This

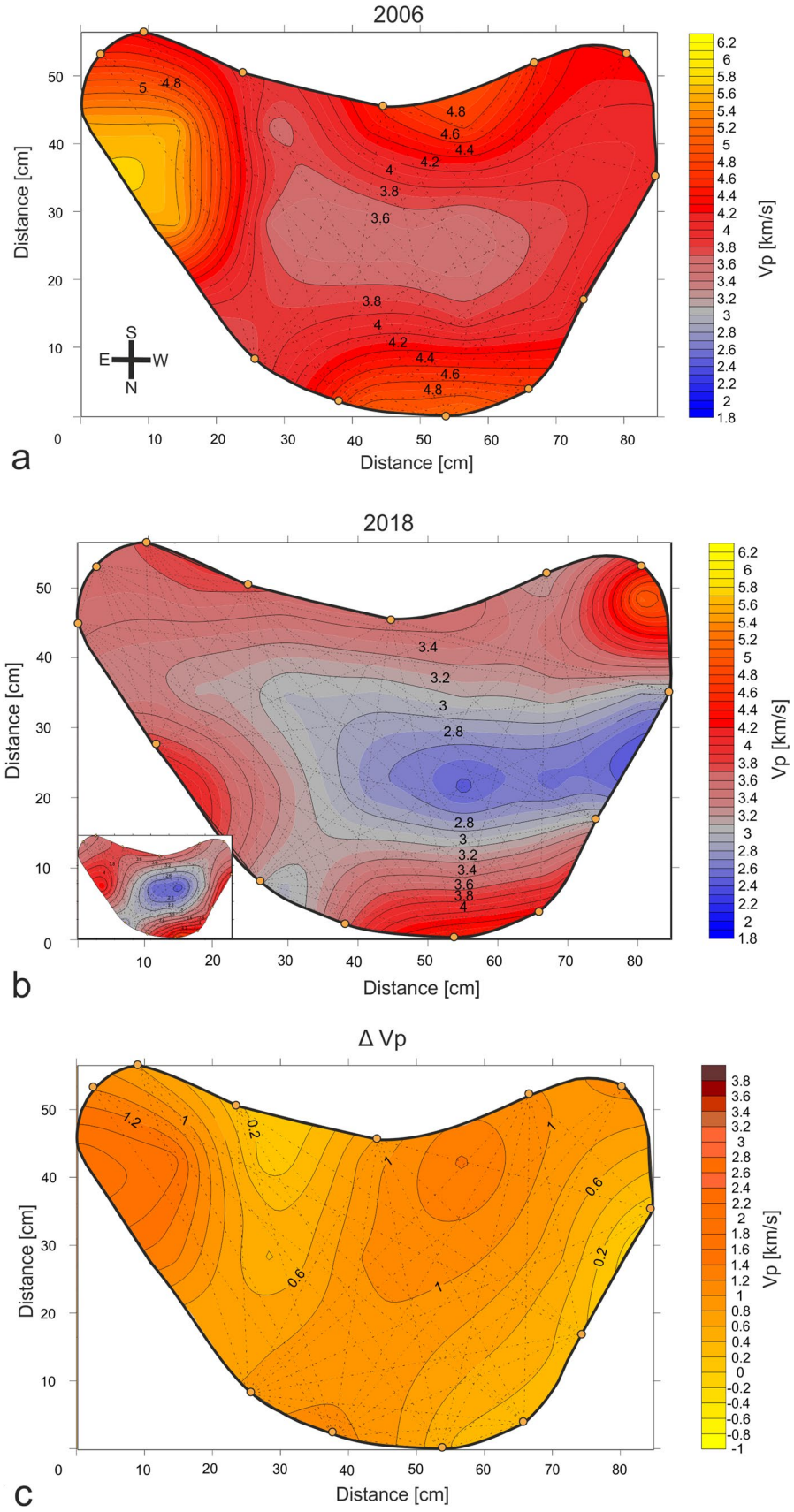

Fig. 13 Ultrasonic tomogram for General v. Bülow measured in **a** 2006, with lower ray coverage, **b** 2018 higher ray coverage and **c** ΔVp modelled by the difference of (**a**) and (**b**), while the amount of rays for the measurement in 2018 was adjusted to the lower amount of rays for the 2006 tomogram (small picture in **b**)

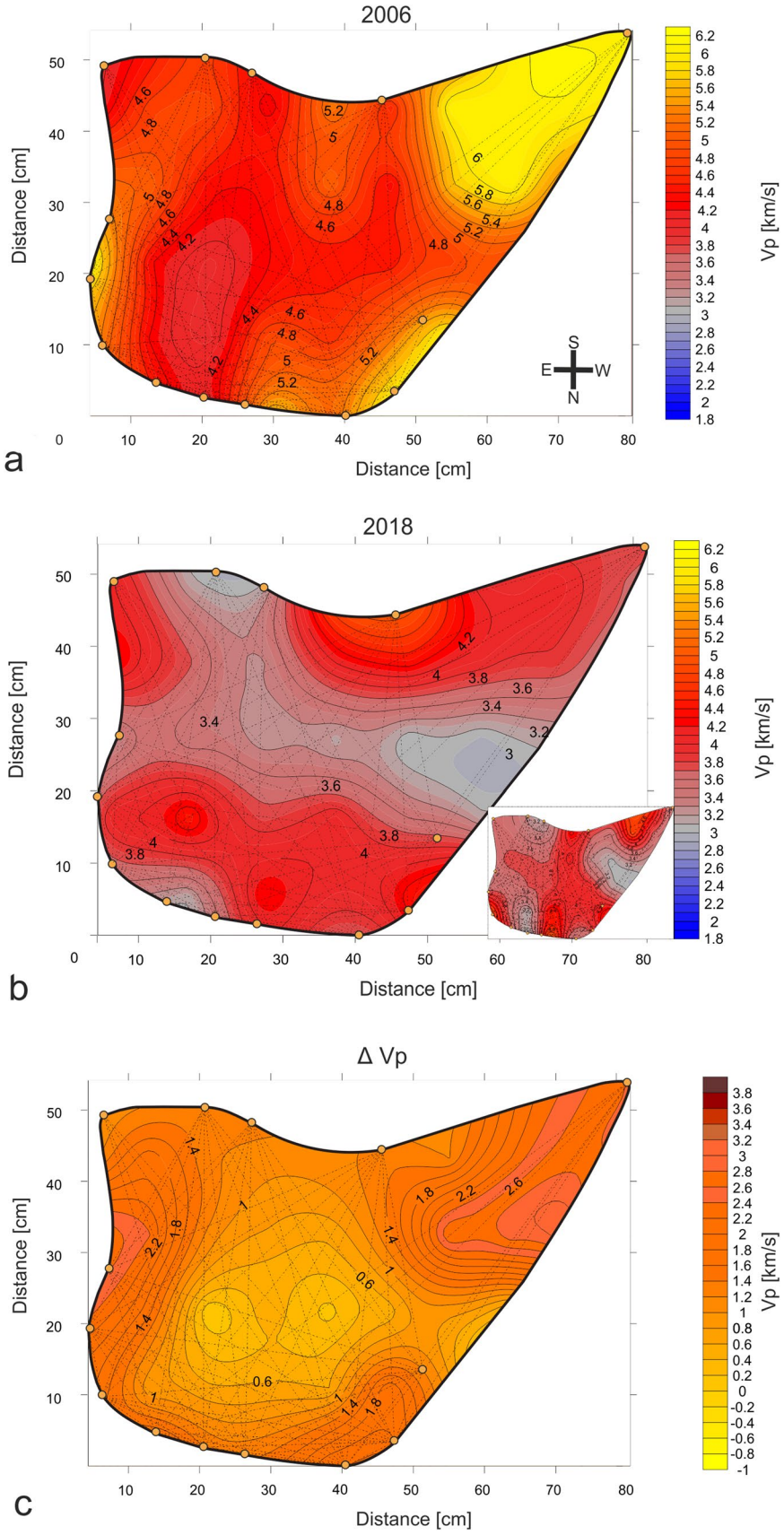

Fig. 14 Ultrasonic tomogram for General v. Scharnhorst measured in **a** 2006, with lower ray coverage, **b** 2018 higher ray coverage and **c** ΔVp modelled by the difference of (**a**) and (**b**), while the amount of rays for the measurement in 2018 was adjusted to the lower amount of rays for the 2006 tomogram (small picture in **b**)

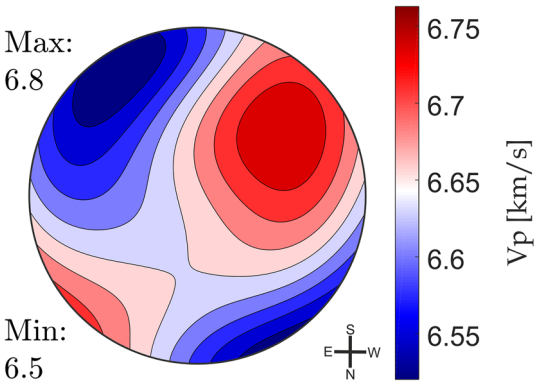

Fig. 15 Reoriented, modelled 3D velocity distribution adjusted to the 2D tomogram of the sculpture von Bülow. The orientation is the same as for the sculpture, see compass direction

trend changes for the absolute reduction measured for the tomogram (grey dots). Here, the reduction increases with a greater thickness of the sculpture. This observation differs from the observations made for Scharnhorst (Fig. 16b), where the results for the tomographic plane show the same distribution, with higher reductions for short travel paths as measured for the different transmission measurements. Moreover, the values for the tomographic layer decreased more notably than for the single measurements. This unexpected result for Bülow may be explained by different reasons. First of all, the total number of measurements for a short distance have been smaller for Bülow in 2006 than for Scharnhorst; therefore, less velocities could be compared for these distances. Another aspect that could influence these results is a consolidation, which was performed in 2006 for the sculptures. Here, 3% Paraloid B72 was applied to optimise the conditions of that sculpture. The high volatility of the used solvent could lead to an enrichment of that consolidation material on the surface. This could also be an explanation for the higher velocities on the surface and the lower velocities in the middle of that sculpture, analysed by the tomogram. The lower velocity could also be strengthened by the influence of the texture, as described above. In contrast to this, the velocities analysed for General von Scharnhorst show a "normal" distribution with lower velocities for short distances and higher velocities for long distances. The velocities for the tomogram show a high reduction, with an average decrease of 1 km/s and a standard deviation of 0.6 km/s. The monument of Bülow shows an average reduction of 0.7 km/s and a standard deviation of 0.3 km/s. Due to the generally worse conditions for Bülow, the deterioration progress slows down as compared to Scharnhorst.

A surprising aspect is the strong velocity decrease since 2006. In 2004, an annual winter sheltering was initiated for both sculptures between November and April; therefore, deterioration increasing effects such as ice crystallisation should not affect the decay anymore. The reasons for the decrease must, therefore, be the ongoing thermohygric deterioration, induced by temperature changes under humid conditions (e.g. Koch and Siegesmund 2004; Menningen et al. 2018a). Another influence can possibly be a higher degree of dryness in 2018, compared to the former measurements, as the sculptures have been covered for three years. The huge influence of humidity to the ultrasonic velocities was reported several times; therefore, this effect cannot be excluded, especially for the thicker parts like the torso.

The degree of deterioration for both sculptures shows an alarming state and therefore, restoration measures need to be undertaken. One possibility could be the application of consolidation materials, which is difficult, as there are several requirements that need to be fulfilled. The consolidation materials need to reach a high penetration depth, which is almost impossible based on conventional application methods as rinsing or the usage of a brush as the marble has a very low water uptake. Another aspect is the material itself. Acrylic resins and their application depths are connected to the used solvent and a possible and very common migration back to the surface as soon as the solvent evaporates. Also, the physical properties of the consolidation material can cause further problems. An alternative could be the application of vacuum induced treatments. In October 2018, the Neptune grotto in Potsdam, Park Sanssouci was reopened after a successful acrylic total impregnation (ATI) by Ibach GmbH (see Lachmann 2019). The use of a modified fluid for the so-called ATI 50 treatment should cause lower thermal expansion as the former formulation, as well as the thermal stress, which occurs during the treatment should be lower (see Sobott and Jbach 2019). Another possibility is the transfer of both sculptures to a museum storage to ensure stable environmental conditions, while the sculptures could be replaced with copies.

In conclusion, the analysis of comparative ultrasonic measurements is a powerful tool for providing a deeper knowledge of the weathering behaviour. The careful and transparent documentation of all measurements was in this context the most important aspect for the comparative studies and allowed to distinguish between irregularities, especially as two sculptures with almost the same conditions could be investigated.

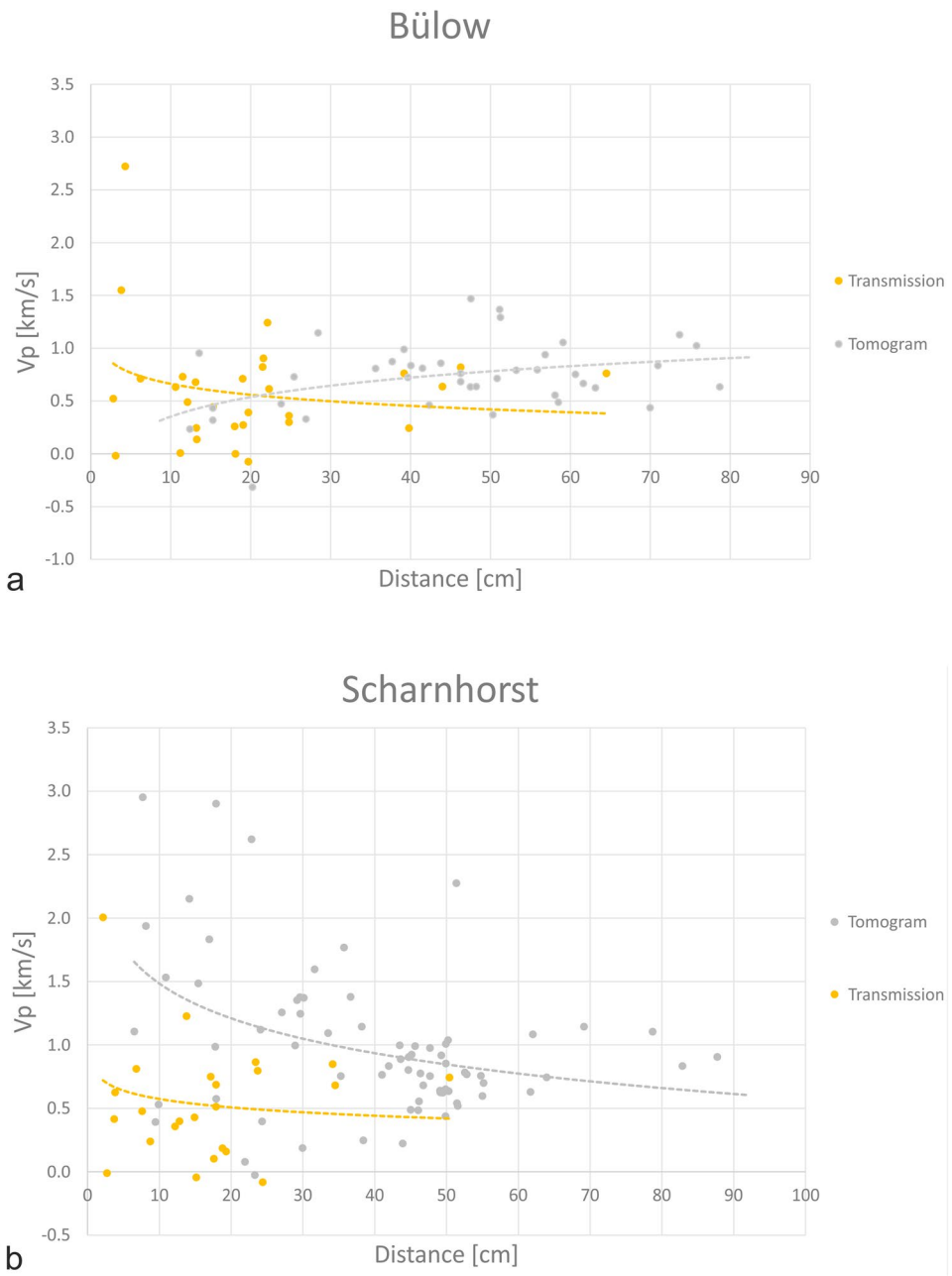

Fig. 16 Difference between the measured ray velocities in 2006 and 2018 (km/s) for von Bülow (**a**) and von Scharnhorst (**b**). The grey dots represent the reductions for the tomogram, while the orange dots represent the transmission measurements, plotted according to the distance (cm) the ray needed to travel

Acknowledgements Open Access funding provided by Projekt DEAL. The authors gratefully acknowledge F. Heidelbach for doing the EBSD measurements and would like to thank D. Mainprice for his help modelling the EBSD data. Our special gratitude goes to S. Kraus und C. Kloss for their great work and patience with the measuring investigation and C. Gross for his patient correction of the sometimes very German English. For their critical and constructive review, we would like to gratefully acknowledge the work of the anonymous reviewer, who helped to improve this work. The study has been supported by the BMBF (Marmorbild FKZ: 03VP00292), which we gratefully acknowledge.

References

Ahmad A, Pamplona M, Simon S (2009) Ultrasonic testing for the investigation and characterization of stone—a non-destructive

and transportable tool. Stud Conserv 54(sup1):43–53. https://doi.org/10.1179/sic.2009.54.Supplement-1.43
Babacan AE, Gelisli K (2015) Ultrasonic investigations of marble columns of historical structures built in two different periods. Carbonates Evaporites 30(3):357–363. https://doi.org/10.1007/s13146-015-0233-x
Bachmann F, Hielscher R, Schaeben H (2010) Texture analysis with MTEX—Free and Open Source Software Toolbox. Solid State Phenom 160:63–68
Blum R, Rahm U (1998) Ultraschall- und Bohrwiderstandsmessungen. In: Die Steinskulpturen am Zentralbau von Schloss Clemenswerth/Emsland, München
Brimblecombe P (2014) Environment and architectural stone. In: Siegesmund S, Snethlage R (eds) Stone in architecture, 5th edn. Springer, Berlin, pp 317–347
Capizzi P, Cosentino PL, Schiavone S (2013) Some tests of 3D ultrasonic traveltime tomography on the Eleonora d'Aragona statue (F. Laurana, 1468). J Appl Geophys 91:14–20
Cardarelli E, de Nardis R (2001) Seismic refraction, isotropic anisotropic seismic tomography on an ancient monument (Antonino and Faustina temple AD 141). Geophys Prospect 49(2):228–240
DBU, final report AZ 29544/01 Labor Köhler (2015) Erarbeitung eines Bewertungs-Leitfadens für Ultraschallmessungen an umweltgeschädigten Marmorskulpturen am Beispiel u. a. des Parks Potsdam Sanssouci (UNESCO-Welterbestätte)
Deutsch, V, Platte, M. Vogt, M, Deutsch WAK, Schuster V (2002) Die Ultraschallprüfung, Band 1 aus der Reihe ZfP kompakt und verständlich, Castell-Verlag Wuppertal
Dürrast H, Siegesmund S, Prasad M (1999) Die Schadensanalyse von Naturwerksteinen mittels Ultraschalldiagnostik: Möglichkeiten und Grenzen. Zeitschrift der deutschen geologischen Gesellschaft, pp 359–374.
Fleischer G (2002) Beurteilung von Ultraschalluntersuchungen an Natursteinobjekten in der Denkmalpflege. Dissertation, TU Wien
GeoTom, LLC (2017) GeoTomCG software is described on the website www.geotom.net and can be purchased from GeoTom through contact information on the website. The user's manual and a demo program are available free from GeoTom
Goretzki L, Füting M, Köhler W (1987) Untersuchungen zur Korrosion der Marmorskulpturen im Park von Potsdam-Sanssouci. Bautenschutz Bausanierung 10(3):104–109
Grunert S (1988) Eine Theorie zu der an Marmorskulpturen beobachteten Innenverwitterung. Abhandlungen des Staatlichen Museums für Mineralogie und Geologie zu Dresden, 35: 95–98
Hielscher R, Schaeben H (2008) A novel pole figure inversion method: specification of the MTEX algorithm. J Appl Crystallogr 41(6):1024–1037
Khazanehdari J, Rutter EH, Casey M, Burlini L (1998) The role of crystallographic fabric in the generation of seismic anisotropy and reflectivity of high strain zones in calcite rocks. J Struct Geol 20(2–3):293–299
Koch A, Siegesmund S (2004) The combined effect of moisture and temperature on the anomalous expansion behaviour of marble. Environ Geol 46(3–4):350–363. https://doi.org/10.1007/s00254-004-1037-9
Köhler W (1988) Preservation problems of Carrara marble sculptures Potsdam-Sanssouci (''radical structural destruction'' of Carrara marble). VI International congress on deterioration and conservation of stone, Proc Actes, pp 653–662
Köhler W (1991) Untersuchungen zu Verwitterungsvorgängen an Carrara-Marmor in Potsdam-Sanssouci.-Berichte zu Forschung und Praxis der Denkmalpflege in Deutschland, Steinschäden—Steinkonservierung 2, Hannover, pp50–53
Köhler W (2014) Erhaltung von Marmorskulpturen unter mitteleuropäischen Umweltbedingungen, Beiträge des 8. Konservierungswissenschaftlichen Kolloquiums in Berlin/Brandenburg. Arbeitshefte des Brandenburgischen Landesamtes für Denkmalpflege und Archäologischen Landesmuseums, Nr. 32, pp. 37–44
Köhler (2018) Ultraschalldiagnostik- ein essentieller Bestandteil bei der Berechnung der Risikoziffer. In: Drewello R (ed) Risikoziffer. Umweltschäden an Marmor und Sandsteinskulpturen erfassen und objektiv bewerten, Bamberg: University of Bamberg Press, Forschungen des Instituts für Archäologie, Denkmalkunde und Kunstgeschichte Abteilung Denkmalkunde, Band 12, pp 65–77
Lachmann F (2019) Die Rückkehr des Meeresgottes, Naturstein 02/2019, pp 42–44
Leiss B, Ullemeyer K (1999) Texture characterisation of carbonate rocks and some implications for the modeling of physical anisotropies, derived from idealized texture types. Zeitschrift der Deutschen Geologischen Gesellschaft 150(2):259–274
Lindner H, Pretzschner C, Rost L (1999) Ultraschalluntersuchungen an Bauwerken. Zeitschrift der Deutschen Geologischen Gesellschaft 150(2):375–386
Luque A, Leiss B, Alvarez-Lloret P, Cultrone G, Siegesmund S, Sebastian E, Cardell C (2011) Potential thermal expansion of calcitic and dolomitic marbles from Andalusia (Spain). J Appl Crystallogr 44(6):1227–1237. https://doi.org/10.1107/S0021889811036910
Mahmutoğlu Y (2017) Prediction of weathering by thermal degradation of a coarse-grained marble using ultrasonic pulse velocity. Environ Earth Sci 76(12):785. https://doi.org/10.1007/s12665-017-6770-y
Mainprice D, Casey M, Schmid S (1990) The seismic properties of Alpine calcite and quartz mylonites determined from the orientation distribution function ECORS-CROP-NFP20-ALPES special volume. Bulletin del la Société Géologique de France 156:85–89
Mainprice D, Hielscher R, Schaeben H (2011) Calculating anisotropic physical properties from texture data using the MTEX open source package. In: Prior DJ, Rutter EH, Tatham DJ (eds) Deformation mechanisms, rheology and tectonics: microstructures, mechanics and anisotropy (Special Publications, 360). Geological Society, London, pp 175–192
Maitland T, Sitzman S (2010) Electron backscatter diffraction (EBSD) technique and materials: characterization examples. In: Zhou W, Scanning ZLW (eds) Microscopy for nanotechnology: techniques and applications. Springer-Verlag, Berlin
Menningen J, Siegesmund Si, Lopes L, Martins R, Sousa L (2018a) The Estremoz marbles: an updated summary on the geological, mineralogical and rock physical characteristics. Environ Earth Sci 77(5):S.53. https://doi.org/10.1007/s12665-018-7328-3
Menningen J, Siegesmund S, Tweeton D, Träupmann M (2018b) Ultrasonic tomography: non-destructive evaluation of the weathering state on a marble obelisk, considering the effects of structural properties. Environ Earth Sci 77(17):S1338. https://doi.org/10.1007/s12665-018-7776-9
Pascale G, Lolli A (2015) Crack assessment in marble sculptures using ultrasonic measurements: laboratory tests and application on the statue of David by Michelangelo. J Cult Herit 16(6):813–821. https://doi.org/10.1016/j.culher.2015.02.005
Rüdrich JM (2003) Gefügekontrollierte Verwitterung natürlicher und konservierter Marmore. Dissertation, University of Göttingen
Rüdrich J, Weiss T, Siegesmund S (2001a) Deterioration characteristics of marbles from the Marmorpalais Potsdam (Germany): a compilation. Zeitschrift der Deutschen Geologischen Gesellschaft 637–663
Rüdrich J, Siegesmund S, Richter D (2001b) Marble columns and their state of weathering: structural evidence and ultrasonic tomography. Zeitschrift der Deutschen Geologischen Gesellschaft, pp 665–680
Rüdrich J, Knell C, Enseleit J, Rieffel Y, Siegesmund S (2013) Stability assessment of marble statuaries of the Schlossbrücke

(Berlin, Germany) based on rock strength measurements and ultrasonic wave velocities. Environ Earth Sci 69:1451–1469

Sáez-Pérez MP, Rodríguez-Gordillo J (2009) Structural and compositional anisotropy in Macael marble (Spain) by ultrasonic, XRD and optical microscopy methods. Constr Build Mater 23(6):2121–2126. https://doi.org/10.1016/j.conbuildmat.2008.10.013

Sobott RJ, Jbach HW (2019) AVT weiterentwickelt, Naturstein 02/2019, pp 45–47

Scheffzük C, Siegesmund S, Nikolayev DI, Hoffmann A (2007) Texture, spatial and orientation dependence of internal strains in marble: a key to understanding the bowing of marble panels? In: Prikryl R, Smith BJ (eds) Building stone decay: from diagnosis to conservation, special publications 271. Geological Society, London, pp 237–249

Shushakova V, Fuller ER Jr, Siegesmund S (2011) Influence of shape fabric and crystal texture on marble degradation phenomena: simulations. Environ Earth Sci 63:1587–1601

Shushakova V, Fuller ER Jr, Siegesmund S (2013) Microcracking in calcite and dolomite marble: microstructural influences and effects on properties. Environ Earth Sci 69(4):1263–1279. https://doi.org/10.1007/s12665-012-1995-2

Siegesmund S, Dürrast H (2014) Physical and mechanical properties of rocks. In: Siegesmund S, Snethlage R (eds) Stone in architecture, 5th edn. Springer-Verlag, Berlin Heidelberg, pp 199–214

Siegesmund S, Weiss T, Vollbrecht A, Ullemeyer K (1999) Marble as natural building stone: rock fabrics, physical and mechanical properties. Zeitschrift der Deutschen Geologischen Gesellschaft 150(2):237–257

Siegesmund S, Weiss T, Rüdrich J (2004) Schadensmonitoring mit Ultraschalldiagnostik: Beispiel Marmorpalais in Potsdam. Restauro Zeitschrift für Kunsttechniken, Restaurierung und Museumsfragen 110(2):98–105

Siegesmund S, Kracke T, Rüdrich J, Schwarzburg R (2009) Jewish cemetery in Hamburg Altona (Germany): state of marble deterioration and provenance. Eng Geol. https://doi.org/10.1016/j.enggeo.2009.07.008

Siegesmund S, Pirskawetz S, Rieffel Y, Gossart E, Joksch U, Weise F, Plagge R, Rüdrich J (2013) Die Schlossbrücke in Berlin-Via Triumphalis. In: Naturstein in der Kulturlandschaft, Siegesmund und Snethlage

Snethlage R (2014) Erhaltung von Marmorskulpturen unter mitteleuropäischen Umweltbedingungen, Beiträge des 8. Konservierungswissenschaftlichen Kolloquiums in Berlin/Brandenburg. Arbeitshefte des Brandenburgischen Landesamtes für Denkmalpflege und Archäologischen Landesmuseums, Nr. 32, pp 21–30

Snethlage R, Ettl H, Sattler L (1999) Ultraschallmessungen an PMMA-getränkten Marmorskulpturen. Zeitschrift der deutschen geologischen Gesellschaft 387–396

Van Wenk HR, Houtte P (2004) Texture and anisotropy. Rep Progress Phys 67(8):S.1367

Wedekind W, Rüdrich J, Rieffel Y, Siegesmund S (2014). Long-term evaluation of the conservation state of marble-statues. Proceedings of the ICOMOS-ISCS International Conference on Conservation of Stone and Earthen Architectural Heritage, May 20–23, 2014, Kongju National University, Gongju, Republic of Korea, pp 35–41

Weiss T, Leiss B, Oppermann H, Siegesmund S (1999) Microfabric of fresh and weathered marbles: implications and consequences for the reconstruction of the Marmorpalais Potsdam. Z dt Geol Ges 150:313–332

Weiss T, Rasolofosaon PN, Siegesmund S (2001) Thermal microcracking in Carrara marble. Zeitschrift der deutschen geologischen Gesellschaft, pp 621–636

Weiss T, Fuller E, Siegesmund S (2002a) Thermal stresses in calcite and dolomite marbles quantified by finite element modelling. In: Siegesmund S, Weiss T, Vollbrecht A (eds) Natural stones, weathering phenomena, conservation strategies and case studies. Geological Society Special Publication, 205, pp 81–94

Weiss T, Rasolofosaon PNJ, Siegesmund S (2002b) Ultrasonic wave velocities as a diagnostic tool for the quality assessment of marble). In: Siegesmund S, Weiss T, Vollbrecht A (eds) Natural stones, weathering phenomena, conservation strategies and case studies. Geological Society Special Publications 205, London, pp 149–164

Wildhalm C, Eppensteiner W, Tschegg E (1999) Meßmethoden zur Beschreibung von Gefügeanisotropien in Marmor. Zeitschrift der deutschen geologischen Gesellschaft 150(2):275–281

Zeisig A, Siegesmund S, Weiss T (2002) Thermal expansion and its control on the durability of marbles. In: Siegesmund S, Weiss T, Vollbrecht A (eds) Natural stones, weathering phenomena, conservation strategies